Design and Realisation of Front-End Circuits at 47 GHz using Additive Printing Technology

A DISSERTATION

Submitted in partial fulfillment of the requirement

for the award of the degree of

MASTER OF TECHNOLOGY

IN

ELECTRONICS AND COMMUNICATION ENGINEERING

(With Specialization in RF and Microwave Engineering)

submitted by

Budhaditya Bhowmick

(17533005)

Department of Electronics and Computer Engineering

Indian Institute of Technology Roorkee

Roorkee – 247667, India

June 2019

CANDIDATE'S DECLARATION

I hereby declare that the dissertation topic **"Design and Realisation of Front-End Circuits at 47 GHz using Additive Printing Technology"**, have done by me under the guidance of **Dr. N.P. Pathak**, in the partial fulfillment of the requirement for the award of the degree of Master of Technology in RF and Microwave Engineering, Electronics and Computer Department, Indian Institute of Technology, Roorkee is my original work. The results submitted in this dissertation report have not been submitted for the award of any other Degree or Diploma.

Date: June, 2019
Place: IIT Roorkee

BUDHADITYA BHOWMICK
Enrollment No. 17533005
RF and Microwave Engineering
Department of ECE, IIT Roorkee

CERTIFICATE

This is to certify that the statement made by the candidate is correct to the best of my knowledge and belief. This is to certify that this dissertation topic**, "Design and Realisation of Front-End Circuits at 47 GHz using Additive Printing Technology"** is an original record of candidate's own work accomplished by him under my guidance and supervision. He has not submitted it for the award of any other degree.

Date: June, 2019
Place: IIT Roorkee

Dr. N. P. PATHAK
Professor
Department of ECE, IIT Roorkee

ACKNOWLEDGEMENT

I will like to thank Dr. N.P. Pathak for his constant support and guidance and also for introducing me to this topic. His approach, ideas, insights and avid counseling regarding the topic was immensely helpful and integral. His inputs in each and every step of this thesis were invaluable.

A big thank you to Rahul Jaiswal, Nidhi Pandit, Arun Kumar Varshney, Arpit Burnwal for their constant guidance and support. I will also like to thank all the scholars in the RFIC lab for helping me in every way possible. I will like to acknowledge my batchmate Lt. Lalit Kumar Saini for motivating me.

I will also like to thank Mr. S.K. Gaur, and all the members of the tinkering lab for their important role during the hardware realisation of the thesis.

In the end I will like to acknowledge my mother Kaberi Bhowmick for her unending patience and support. A huge thank you to my sisters Shreya Bhowmick and Preitha Mazumdar for constantly encouraging me.

Budhaditya Bhowmick

ABSTRACT

This dissertation deals with the simulation, design, analysis of Non-Radiative Dielectric (NRD) guide based circuits and NRD transitions. NRD guide is a type of waveguide where a dielectric strip is kept between two metal plates separated by distance less than the half of the free space wavelength. Here Polylactic Acid (PLA) is used as the dielectric medium which is used as a cartridge in 3D printing. PLA is a type of bio-plastic which are basically plastics derived from biodegradable mass.One of the striking features of PLA is that it is biodegradable.The advantages and shortcomings of PLA have been discussed in detail. The electrical properties of PLA are mainly focussed where the low S21 values in the transition structures were attributed to high dielectric loss tangent value of PLA. In this thesis all the simulations were done using FEM simulator HFSS. The NRD transitions such as NRD to waveguide transitions, NRD to waveguide transition using horn antenna with E-plane flared and H-plane tapered, NRD to microstrip transition have been simulated. All the transition structures are analyzed with main focus around 47 GHz. The design and analysis of transition structures are of utmost importance so that NRD guide based circuits can be designed in the future. A bandpass filter and bandstop filter using NRD to waveguide transition were designed and simulated with a centre frequency of 47GHz. NRD to microstrip transition has been realized physically and the experimental results are discussed in detail. The shortcomings and their solutions have also been discussed. The field lines and propagation of different modes of the NRD structures have also been analyzed and solutions are provided if anomalies were found regarding it.

CONTENTS

LIST OF TABLES

LIST OF FIGURES

Chapter 1: Introduction

1.1 Background

Huge development in the communication sector has been observed over the past few decades. Conventional frequency bands included in the RF and Microwave have practically been filled up. So Millimetre wave bands are used for developing new technologies [1]. Millimetre wave bands include frequencies from 30 GHz to 300Ghz. Main advantages of using Millimetre wave includes:

i. Possibility of reusing frequencies.
ii. Smaller in size and light weighted structures are used.
iii. Higher capacity and higher resolution.

Generally technologies used in this region is categorised in two divisions wiz: Planar and Non-Planar technologies. Planar technologies are divided in 3 categories wiz: Microwave Integrated-Circuits (MIC), Miniaturized-Hybrid-Microwave-Integrated-Circuits (MHMIC), and Monolithic-Microwave-Integrated-Circuits (MMIC) [2], [3]. Non-Planar technologies is categorised in two divisions wiz: Metallic waveguides and dielectric waveguides.

1.2 Motivation

Usually planar guided structures include microstrip lines for circuits used in microwave region [4]. It is widely used in planar guided structure as mounting of lumped elements can be done easily in series configuration. Major shortcomings include high losses in transmission, high dispersion in shunt configuration. To overcome this slot-line and coplanar structures were proposed [5]. These planar structures failed to provide satisfactory results at millimetre waves due to their high loss factors as conduction loss become significantly high after 20 GHz [6]. The non-planar structures which include metallic guides also faces the same problem as planar guided structures in millimetre waves and their integrated structures are bulky in nature. As a result they can only be used in structures where low integration is needed. So dielectric guided structures come into picture where one of the main advantages include low losses in transmission but one of the main

disadvantage of these guides is high radiation losses at bends and discontinuities. Hence to overcome these shortcomings Non-Radiative Dielectric guides come into the picture. Different dielectric guides are shown in figure 1.1.

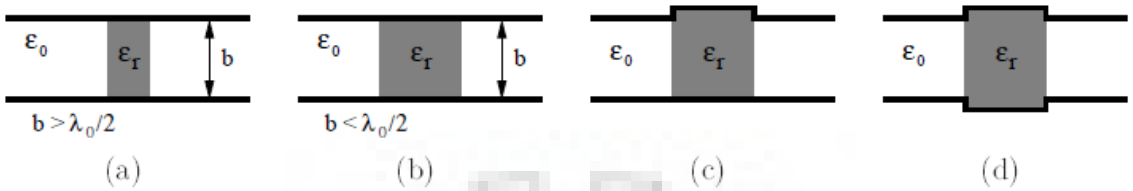

Figure1.1: Different Dielectric guides: (a) H-guide (b) NRD-guide (c) AGNRD-guide (Asymmetrically grooved NRD-guide)[7] (d) hyper NRD-guide [8]

1.3 Non-Radiative Dielectric (NRD) Guide

T. Yoneyama and S.Nishida first proposed Non-Radiative Dielectric (NRD) Guide in 1981. It consists of 2 metal plates which are separated by a distance less than half the free space wavelength by a dielectric strip [9]. The pictorial representation is shown figure 1.2 below.

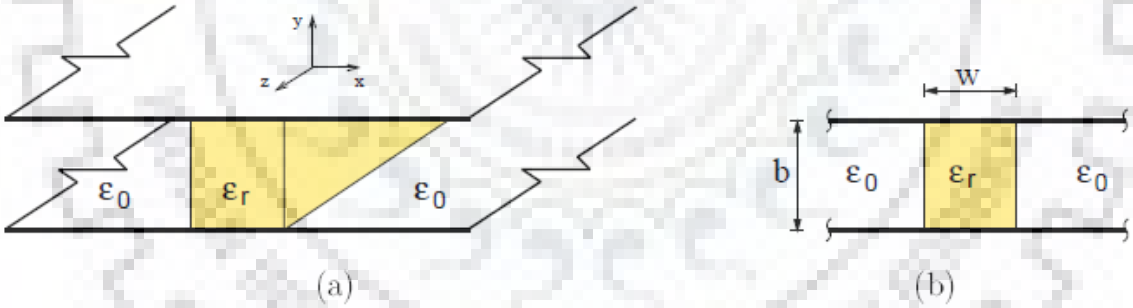

Figure 1.2: NRD-guide: (a) general view, (b) cross section.

In conventional parallel plate waveguide the waves having wavelength higher than half the free space wavelength λ_0 are attenuated hence they are not guided. For this reason in NRD-guide the plate separation is less than $\lambda_0/2$. The propagation condition of the dielectric strip which is placed between the two metallic plate changes locally, so in the air-filled region the wave gets attenuated and in the strip it easily gets guided. In the midway between the 2 metal plates the incoming fields should show symmetry exhibiting Perfect Magnetic Conductor (PMC).

It allows two modes LSE10 mode and LSM11 mode to propagate. In the LSE10 mode the Electric(E) field lines are at 90° with the Non-Radiative Dielectric ground plane [10]. So it is considered to be parasitic and undesirable. So LSM11 mode is the required mode where the Electric(E) field lines are parallel to the ground plane of the guided structure. The propagating modes are shown in Figure 1.3.

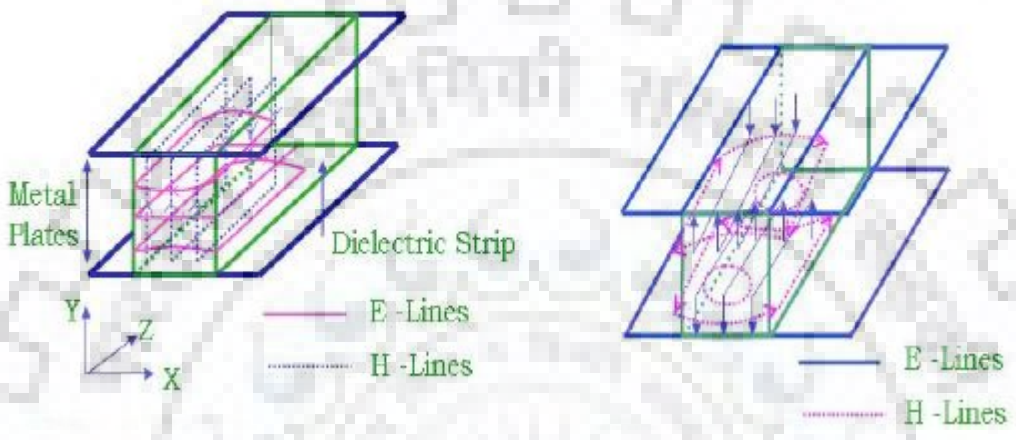

(a) **(b)**

Figure 1.3 Propagating modes of NRD guide (a) LSM11 mode (b) LSE10 mode

1.4 Mathematical Analysis of Non-Radiative Dielectric (NRD) Guide:

To start off we will consider a straight single dielectric. Let the dielectric strip width be a, thickness b, relative dielectric constant be ε_r. Here the analysis is accommodated with the purview that hybrid modes in the NRD guide can be seen as resulting from TM surface waves which propagates in the infinite slab of the same material and same thickness of the dielectric rod and bouncing back and forth between the sidewalls. The cutoff of the strip is given by [11]

$$\lambda_{wgn} = 2a \quad \text{where n=0,1,…} \qquad (1.1).$$

Here λ_{wgn} is the guide wavelength of TM_n slab mode.

$$\lambda_{wgn} = \frac{\lambda_0}{\sqrt{\varepsilon_r - (\lambda_0 * q_n/2\pi)^2}} \qquad (1.2).$$

Here λ_0 is the wavelength in free space and qn is the nth solution of the characteristic equation derived in [12].

$$\frac{q_n}{\varepsilon_r}\tan\left(\frac{q_n b}{2}\right) - \sqrt{(\varepsilon_r - 1)\left(\frac{2\pi}{\lambda_0}\right)^2 - {q_n}^2} = 0, \quad \text{where n is even} \qquad (1.3).$$

$$\frac{q_n}{\varepsilon_r}\cot\left(\frac{q_n b}{2}\right) - \sqrt{(\varepsilon_r - 1)\left(\frac{2\pi}{\lambda_0}\right)^2 - {q_n}^2} = 0, \quad \text{where n is odd} \qquad (1.4).$$

From equation (1.1), single mode operation condition is given as

$$\lambda_0, \lambda_{wg1} > 2a > \lambda_{wg0} \qquad (1.5).$$

Here λ_{wg0} and λ_{wg1} are the wavelengths of the guide at fundamental and second TM slab modes. The region which is bounded by λ_{wg0}=2a and λ_{wg1}=2a and by the upright line a/ λ_0 =0.5.

1.5 Polylactic Acid (PLA)

It is a type of bio-plastic which are basically plastics derived from biodegradable mass. It is derived from corn starch or sugar cane which is a renewable resource. One of the striking features of PLA is that it is biodegradable. In this day and age climate change is of paramount importance and any material which replaces traditional materials which has an adverse effect to the environment like Teflon should be investigated properly to have a cleaner future. In this thesis use of PLA as a dielectric strip is discussed. The electrical properties of PLA are given below:

i) Electrical permittivity: 2.7.
ii) Loss tangent: 0.008.

1.6 Problem Statement

Dissertation objective includes:

I. To observe transmission and reflection characteristics of NRD guide for waveguide, horn and microstrip transitions.
II. To design bandpass filter and bandstop filter using NRD guide.
III. To investigate PLA as a dielectric medium as an alternative to Teflon.

1.7 Organization of Thesis

Chapter 1 discusses the status of circuits in millimetre wave, motivation for NRD based circuits, principle of operation of NRD guide, Polylactic Acid and its electrical properties.

Chapter 2 discusses about the previous work done in NRD, NRD based circuits and transitions.

Chapter 3 discusses about the field lines, propagation of NRD based circuits.

Chapter 4 discusses the NRD to waveguide transitions and NRD based circuits using NRD to waveguide transitions and the simulation result obtained from it.

Chapter 5 discusses the NRD to waveguide transitions with horn antenna and the simulation result obtained from it.

Chapter 6 discusses the NRD to microstrip transition and the simulation and experimental results obtained from it.

Chapter 7 summarizes all the results obtained and discusses about the future scope of this thesis.

Chapter 2: Literature Review

The idea of Non-Radiative dielectric waveguide was presented by T. Yoneyama and S. Nishida [9]. The advantages of using a NRD guide were discussed over traditional guides like insular guides [13], image guides [14], H-guides [11]. At discontinuities and bends decaying of radiated waves and free propagation of the waves in the dielectric strip were cited as main advantages over traditional guided structures. Loss in transmission, BW(Bandwidth) for single mode operation, coupling coefficient were discussed. T junctions, Bends, couplers were implemented and promising results were shown. In THz(terahertz) region transmission characteristics of NRD(non-radiative dielectric) guide was discussed in [15]. Design constraints such as separation between two metal plates of the NRD guide and width of the NRD guide were discussed [16]. The height of the dielectric strip of the NRD guide should be nearly equal to $0.45\lambda_0$ while the width should be in the range of $(0.4\sim 0.6)*\frac{\lambda 0}{\sqrt{\epsilon_r - 1}}$. Main purpose of this paper was to observe the transmission characteristics and compare it with a traditional guide like Co-planar guide at frequency 1.5 THz. Comparison of transmission loss was made between the aforementioned guide and NRD guide were the NRD guide showed low losses as compared to the other guide [17].

For practical use of NRD guide different types of NRD guide transitions have been used over the years. Waveguide transition with tapered dielectric structure was first introduced in J. A. G. Malharbe, et-al in 1984 [18]. Here a standard waveguide working in the X-band was used for transition. The reflection coefficient of the tapered structure was observed and the different parameters like impedance at different position of the tapered strip. Proper matching of the transition structure was stressed to obtain optimum result. S. Mbe Emane, et-al [19] took it forward and designed the aforementioned transition for millimetre wave. Conventional waveguides used for frequencies 30-40 GHz and 45-55 GHz were used and their S21 and S11 values for the above mentioned frequency bands were assessed. The authors made an astute observation that the both the height and width matching of the NRD guide with the waveguide's height and width is of utmost importance for good result .From the results it was concluded that this NRD transition can be used for multi-beam system as mentioned in [20].

T. Yoneyama took a different approach and used horn as transition instead of a waveguide [21]. Like [19] even here a tapered dielectric strip is inserted in the transition part. A customised horn was used where the H-plane is tapered and E-plane is flared. Malherbe represented similar type of

transition which was composite natured [22], where Electric(E) field matching of NRD and horn was done. The tapered length was kept constant at $5\lambda_{wg}$ and rest of the parameters were varied.

Micro-strip transitions have also been used. The main principle involved in this transition technique is aperture coupling [23]-[25]. In the micro-strip transition reported by L. Han, et-al [26] both the dielectric strip and micro-strip line have a common ground plane. For coupling the slots are made on the ground plane. The slots are at an angle 90° with the micro-strip line and parallel to the dielectric strip. Further optimization of the aforementioned design was done [27] where the reflection coefficient(S11) and transmission coefficient(S21) due to variation of the open ends of the micro-strip and coupling slots were observed. Even different types of slots were used and were simulated to obtain optimized results. Further improvements were made in [28] where a metallic mode suppressors were used to nullify unwanted modes and improve reflection coefficient(S11) and transmission coefficient(S21) over the desired band of frequency of the transition.

NRD guide based circuits such as band-pass filter and band-stop filter showed positive outcomes as well. First band-pass filter which used gap coupling was reported in [29]. Realization of band-stop filter using NRD guide is difficult but band-stop filter using dielectric stub configurations have been reported in [30]-[31]. A band-stop at 33.5GHz filter with suspended strip-line transition has been reported in [32].

Chapter 3: Simulation and Analysis of NRD based circuits

3.1 Introduction:

Initial simulations were done without transitions using HFSS software to determine whether the results were promising enough for practical realization. For ease of computation NRD guide with magnetic walls (for symmetry) is used. Due to this symmetry only the bottom half is simulated. PLA (Polylactic acid) is used as the dielectric strip. The relative permittivity is taken as 2.7 with 0.008 loss tangent. The basic structure of a NRD waveguide with magnetic wall is shown in figure 3.1.

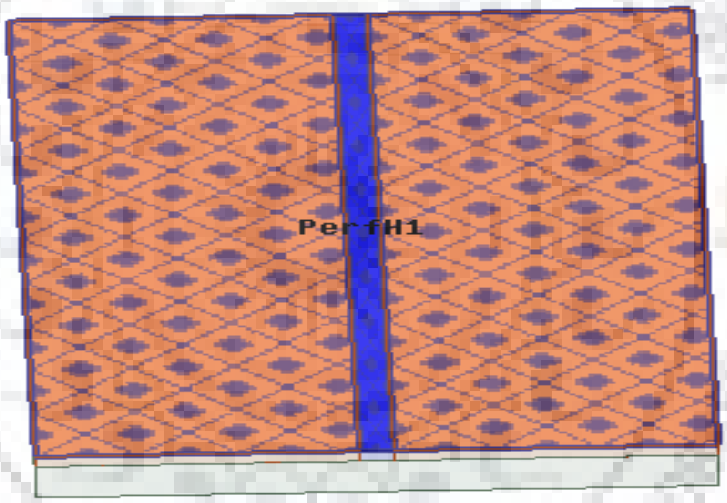

Figure 3.1 Basic structure of NRD guide.

3.2 Variation of separation between the metal plates:

The optimum gap between the plates should be greater than λg/2 and lesser than λ0/2. The center frequency is considered to be 47 GHz. So the optimum gap b should be between 1.97mm to 3.24 mm. Our main target is to have high attenuation and low propagation for any modes higher than 2 and low attenuation and high propagation for modes 1 and 2. Mode 1 is still considered to be

parasitic mode while mode 2 is our desired mode. The dispersion plot of propagation values for different gaps and modes are shown below where the x axis denotes the frequency and y axis denotes the propagation constant:

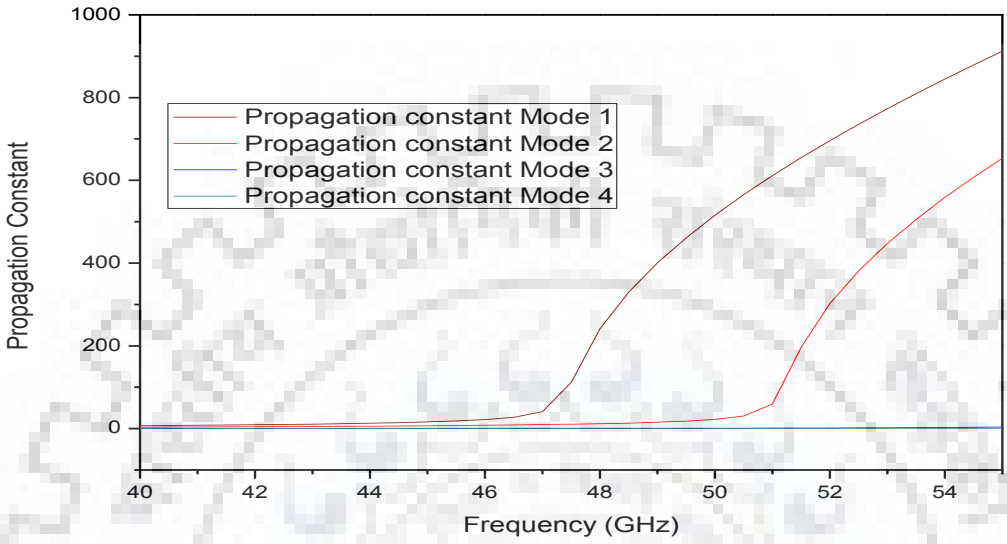

Fig 3.2: Dispersion plot for 1.2 mm gap NRD guide

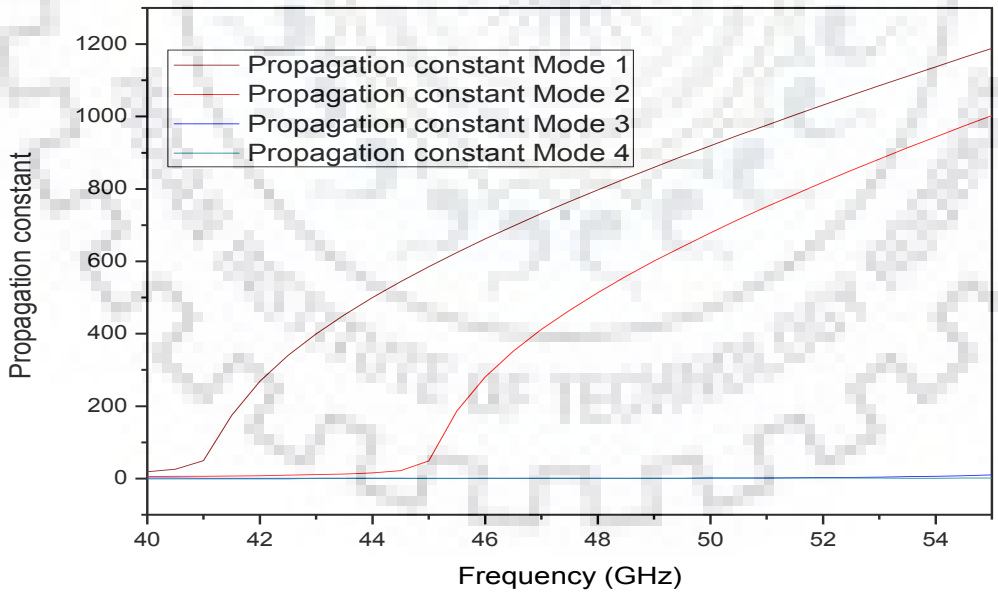

Fig 3.3: Dispersion plot for 1.3 mm width of dielectric strip

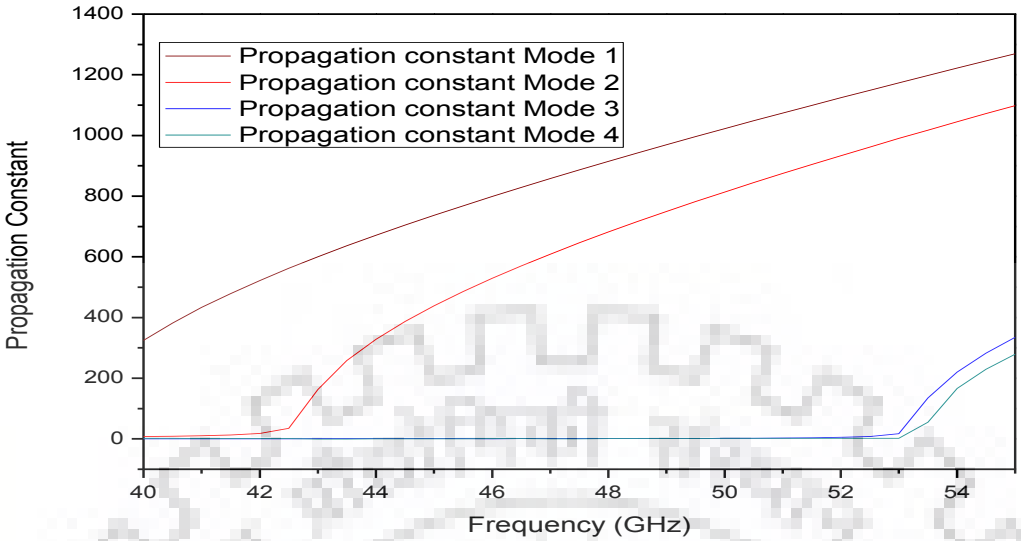

Fig 3.4: Dispersion plot for 1.4 mm gap NRD guide

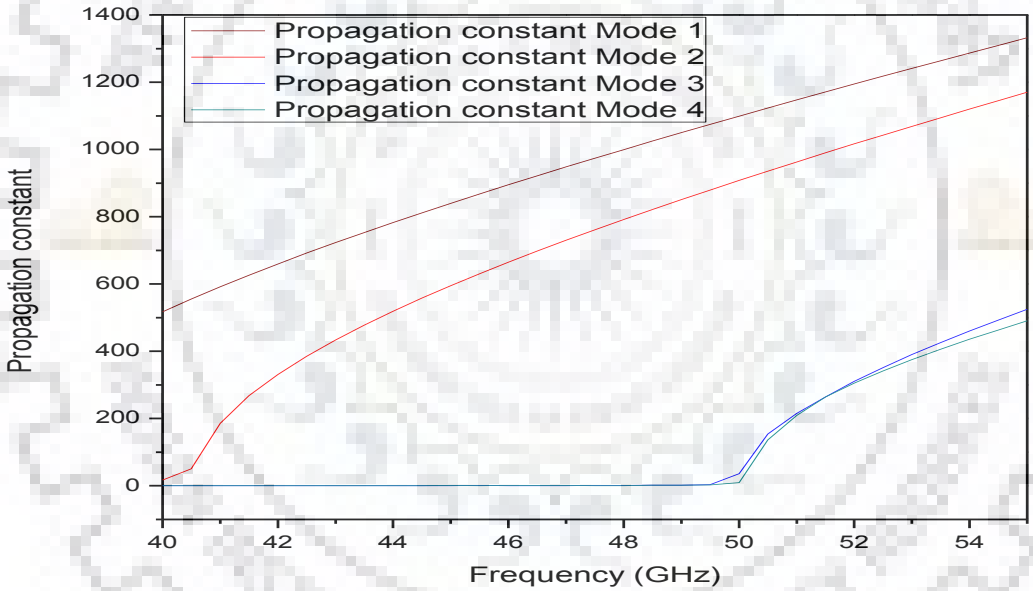

Fig 3.5: Dispersion plot for 1.5 mm gap NRD guide

It should be noted that in all the simulations width of the dielectric strip was fixed at 2.3mm. From the above results it can be seen that on increasing the gap the value of propagation constant increases. For getting a proper propagation constant (β) for mode 2 which is our desired mode the optimum gap between the 2 plates is considered to be 2.6m (1.3 mm half length) based on the dispersion plots as it shows low attenuation and high propagation constant value for modes 1 and 2 and low propagation and high attenuation for other higher modes.

3.3 Variation of width of dielectric strip:

To fine-tune our results even further dispersion plot for different width of the dielectric strip were observed. The dispersion plots are given below.

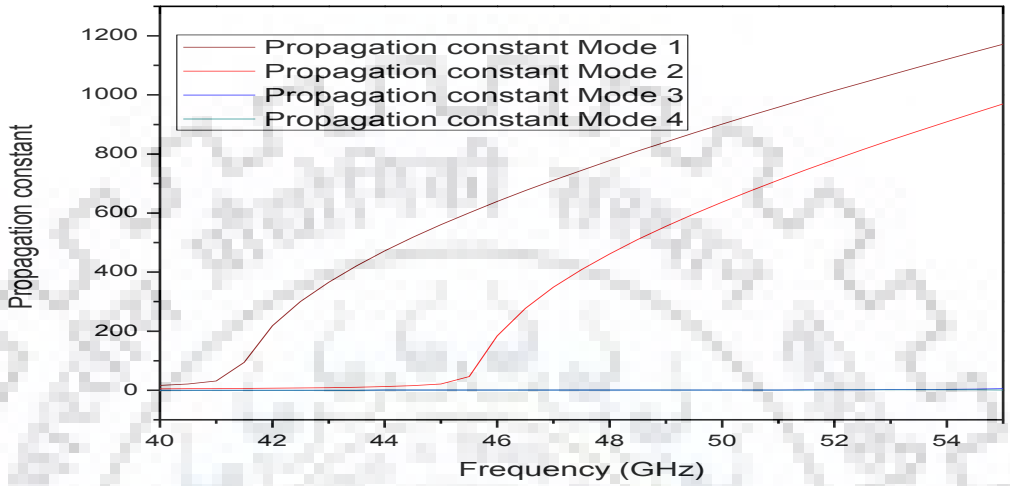

Fig 3.6: Dispersion plot for 2.2 mm width of dielectric strip

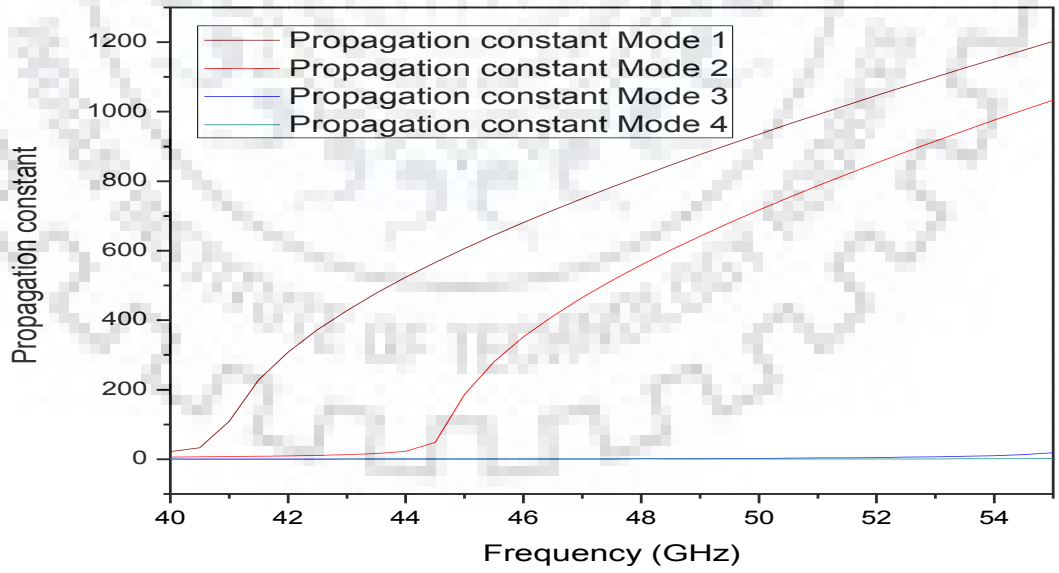

Fig 3.7: Dispersion plot for 2.4 mm width of dielectric strip

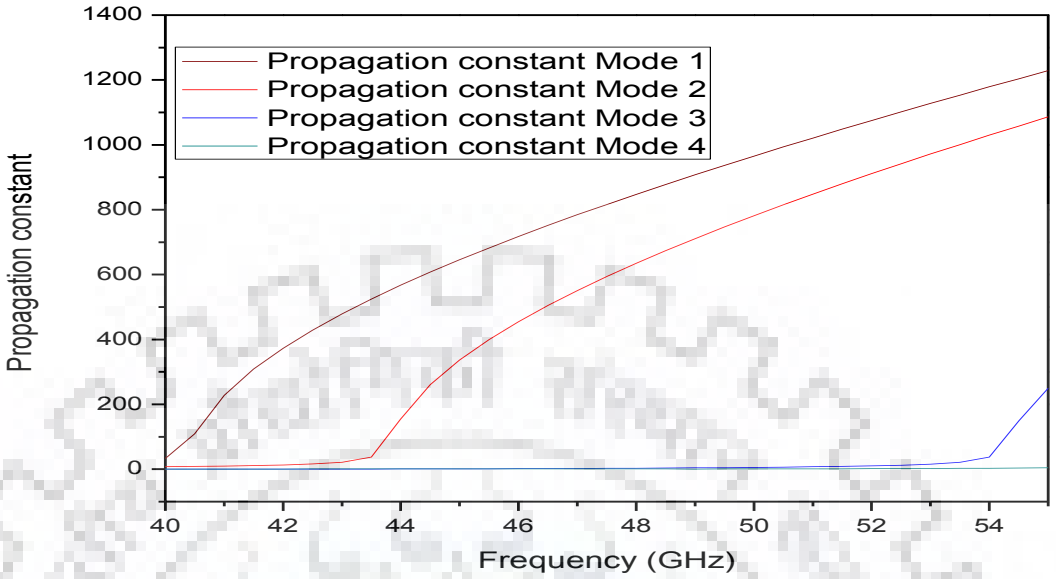

Fig 3.8: Dispersion plot for 2.6 mm width of dielectric strip

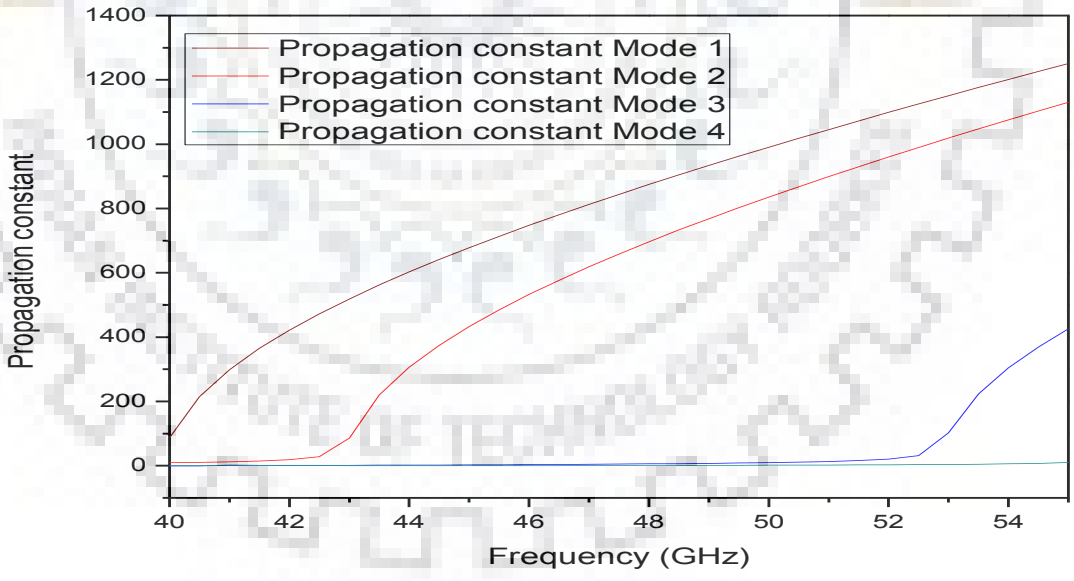

Fig 3.9: Dispersion plot for 2.8 mm width of dielectric strip

Based on the simulation results both the optimum width and height is taken as 2.6mm. The gamma values at different mode for this configuration for port 1 at 47GHz are shown in the table 3.1.

Mode Number	Attenuation	Propagation
1	11.495	784.44
2	13.2	551.3
3	691.45	2.253
4	802.61	0.7525

Table 3.1: Gamma values for different modes at port1 at 47GHz frequency.

The main purpose of these simulations was to obtain the configurations for which only first two modes are allowed to pass in the NRD guide.

3.4 Band-pass Filter Design and analysis:

Now a simple band-pass filter is proposed having structure shown below:

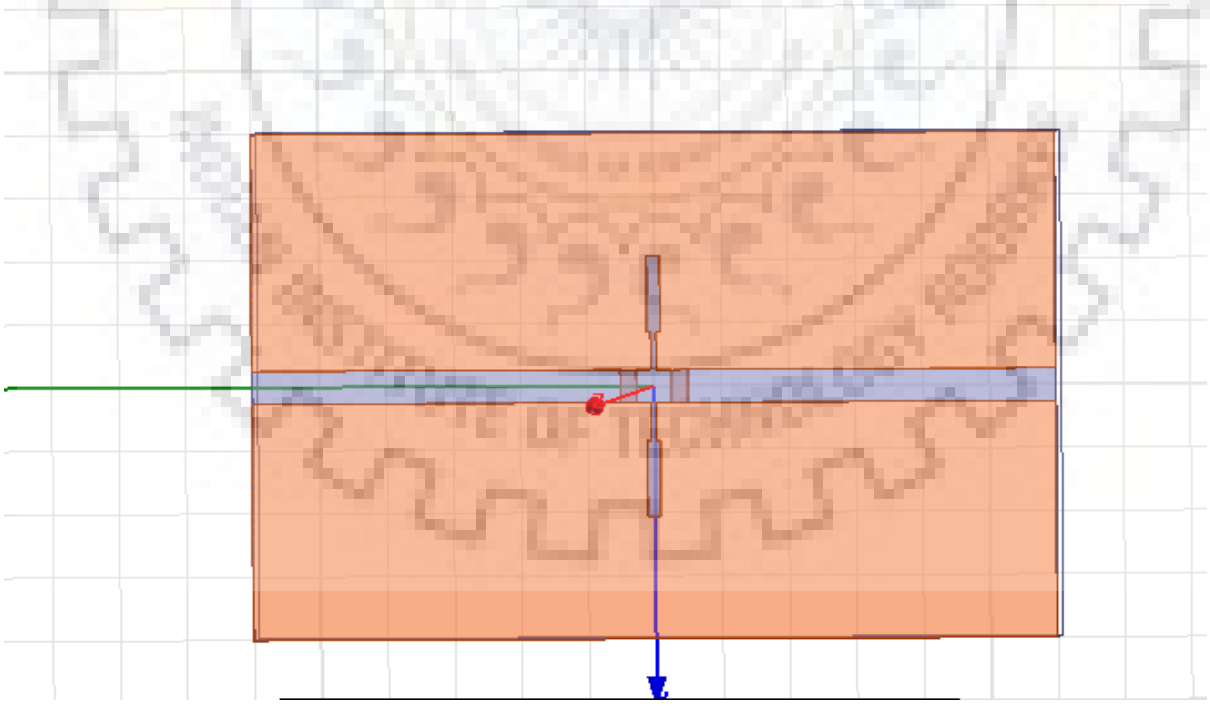

Fig 3.10: Top-view of Single element band-pass filter

The different dimension of the structure is given below.

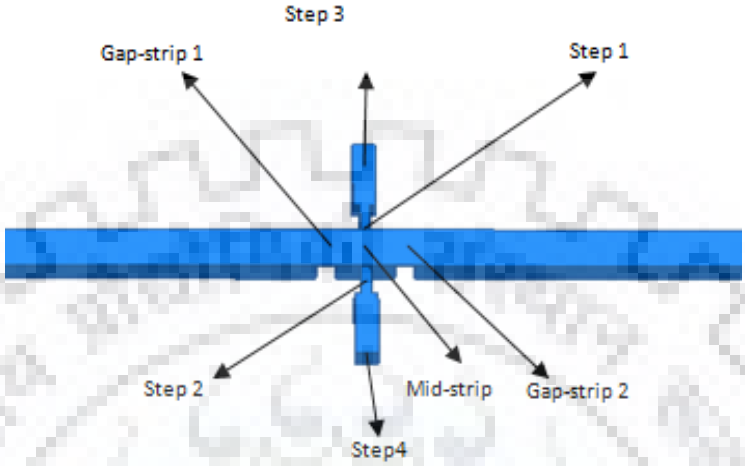

Figure 3.11: Top view of dielectric strip of Single element filter.

Structure name	X-dimension (mm)	Y-dimension (mm)	Z-dimension (mm)
Step 1,Step 2	0.4	6	1 (0.3 mm above lower metal plate)
Step 3,Step 4	1	6	1 (0.3 mm above lower metal plate)
Gap-strip 1, Gap-strip 2	1.2	2.6	0.1
Mid strip	2.6	2.6	1.3

Table 3.2: Dimension of the Single element bandpass filter

The height of the structure is 1.3mm.The S11 and S21 plots are given below:

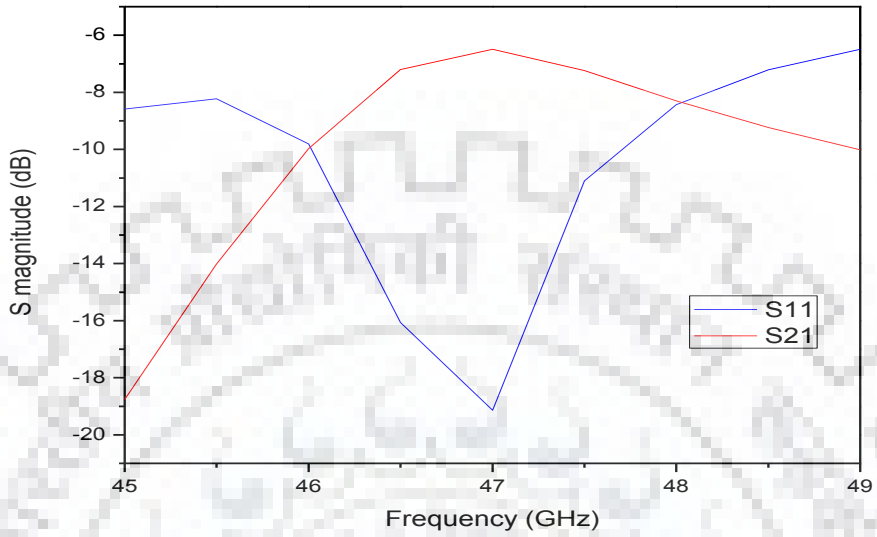

Fig 3.12: S11 and S21 plot for frequencies 45-49 GHz single element band-pass filter

In figure 3.10 the S21 value at center frequency 47GHz is quite low. Moreover the passband is not sharp enough. Now a 3 element periodic structure is used to improve the above result. The top view & the different dimensions of the structure are shown:

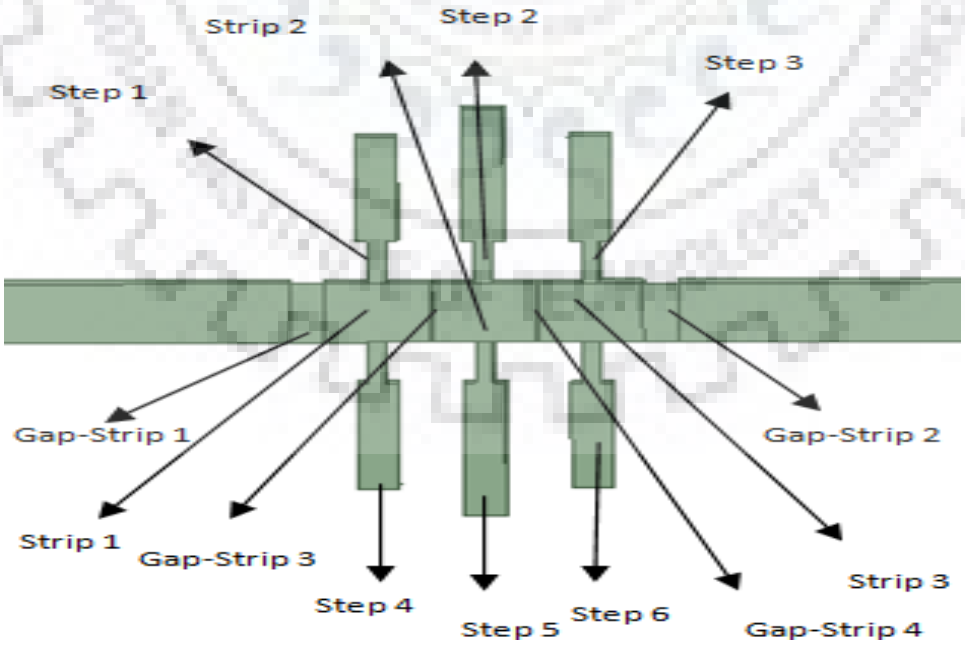

Fig 3.13: Top view of 3 element Band-pass filter

Structure name	X-dimension (mm)	Y-dimension (mm)	Z-dimension (mm)
Step 2	0.4	4	1 (0.3 mm above lower metal plate)
Step 1, Step 3	0.4	3	1 (0.3 mm above lower metal plate)
Step 5	1	6	1 (0.3 mm above lower metal plate)
Step 4, Step 6	1	5	1 (0.3 mm above lower metal plate)
Gap-strip 1, Gap-strip 2	0.1	2.6	0.1
Gap-strip 1, Gap-strip 2	1.2	2.6	0.1
Strip 1, Strip 2, Strip 3	2.6	2.6	1.3

Table 3.3: Dimension of the 3 element bandpass filter

The remaining part of the strip length on either side of gap-strip 1 and gapstrip 2 is 24.8 mm.

The S11 and S22 plot for the frequency range 45-49 GHz is depicted below:

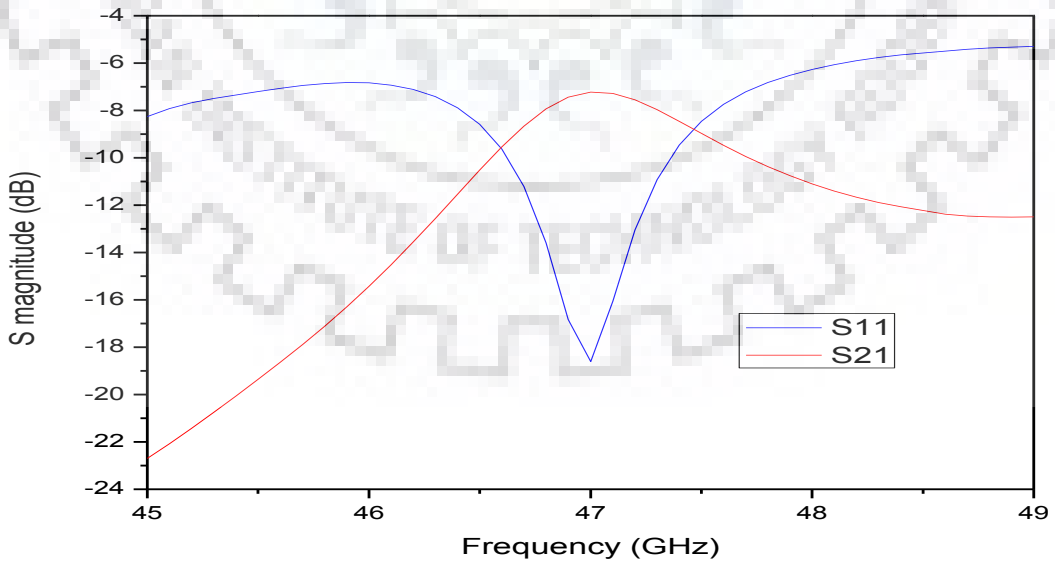

Fig 3.14: S11 and S21 plot for frequencies 45-49 GHz 3-element band-pass filter

From figure 3.14 it is evident that the passband characteristic of the filter has improved considerably from the single element band-pass filter. The S11 is -18.61 dB and S21 is -7.22 dB at 47GHz which is the centre frequency. To further improve the S21 values we can place a thin arlon sheet of width 0.136 mm in between the PLA strips. This sheet has a low loss tangent value (0.0009) and a relative permittivity of 2.2. But the practical realization of placing the arlon sheet is not feasible as the thin sheet needs to be pasted which has its own complications. So this idea was discarded.

3.5 Conclusion

From the simulations it is quite evident that the S21 values are quite low. This is mainly due to the high loss tangent value of 0.008 the dielectric strip PLA. For a low loss tangent value the S21 value will drastically improve which will be shown in the next chapters. The S11 and S22 plots slightly resemble band-pass filter characteristics. The results are promising enough to be implemented practically by using various transitions like waveguide, horn and micro-strip which will be shown in the next chapters.

Chapter 4: Simulation and Analysis of NRD based millimetre wave circuits using NRD to Waveguide transition

4.1 NRD to Waveguide transition

Waveguide transition was first reported in [18] by J. A. G. Malharbe, et-al in 1984 where a tapered dielectric structure was used as the NRD strip. Now in this transition only one mode is allowed to propagate. The width and height of the tapered section and the waveguide is of utmost importance to achieve proper matching. Here the waveguide transition was made to operate from 44 to 50 GHz frequency with main focus around 47 GHz as other NRD based circuits will be simulated with 47 GHz as the centre frequency. The main objective of the transition structure is to have low S11 values and S21 values for the entire frequency region. The simulation setup is shown in fig 4.1. Simulations were done in HFSS 17.1.

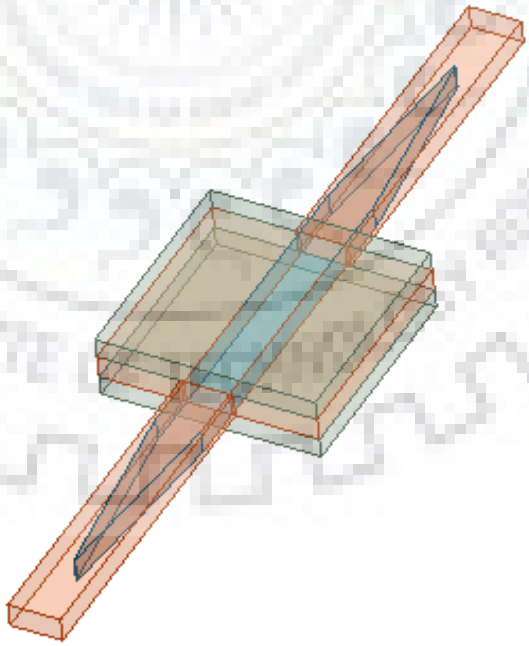

Fig 4.1: Simulation setup for waveguide to NRD transition

The S11 and S21 plot for variation of width of the dielectric strip made up of PLA where height is fixed at 2.35mm is shown below:

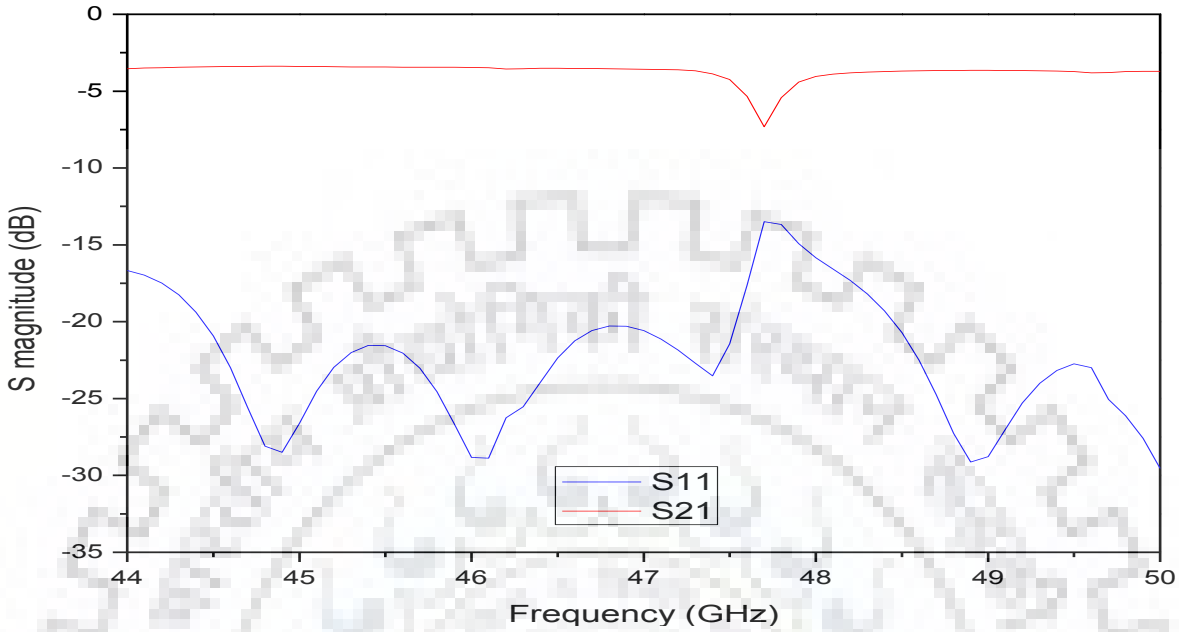

Fig 4.2: S11 and S21 plot for frequencies 44-50 GHz of Waveguide to NRD transition for 4 mm width of dielectric strip

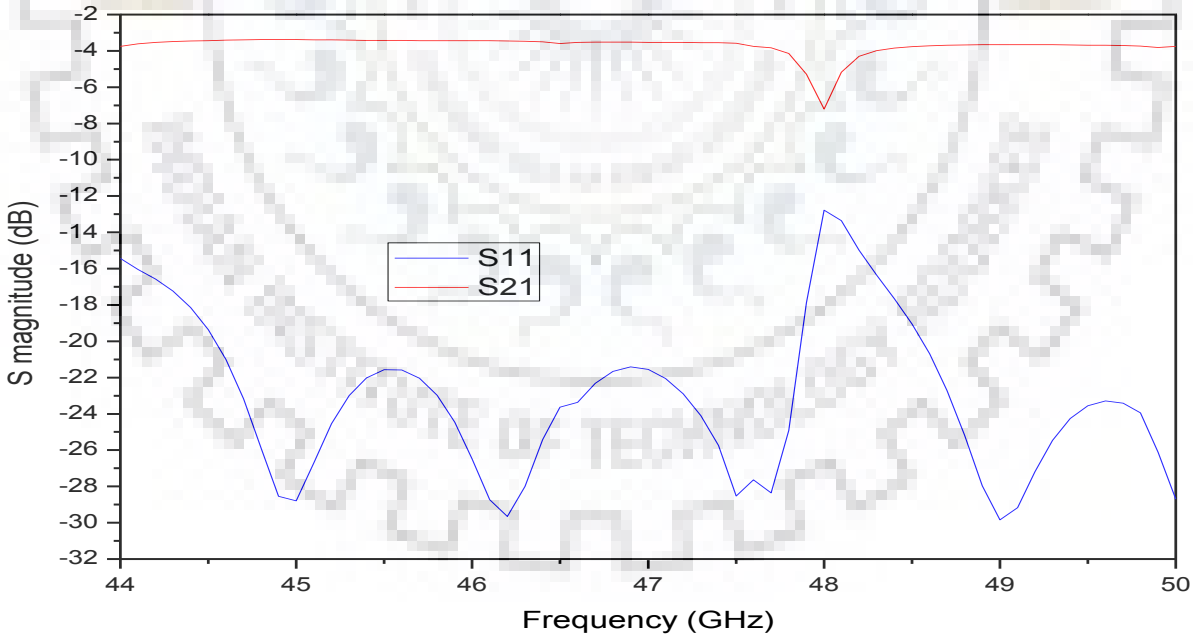

Fig 4.3: S11 and S21 plot for frequencies 44-50 GHz of Waveguide to NRD transition for 4.1mm width of dielectric strip

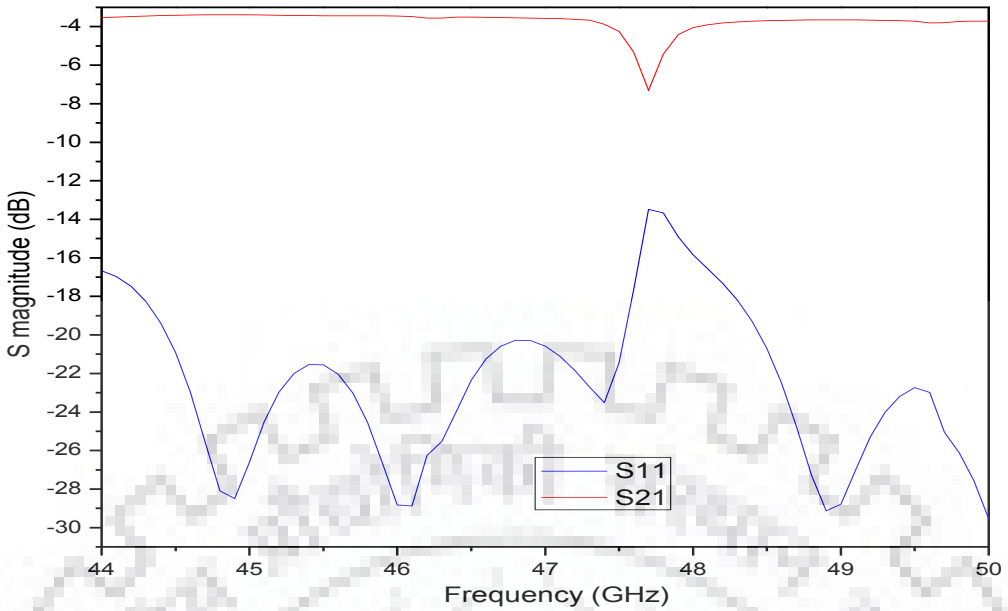

Fig 4.4: S11 and S21 plot for frequencies 44-50 GHz of Waveguide to NRD transition for 4.2mm width of dielectric strip

From the above results 4.1mm width dielectric strip was considered to be the optimum width. The S11 does not exceed -15dB except at 48 GHz in the entire frequency range which shows good matching and the S21 remains nearly constant at 3.5dB for almost the entire frequency range except at 48 GHz which is due to discontinuities in the structure. It should be noted that the height and breadth of the waveguide used in simulation is same as that of a standard WR22 waveguide. The propagation and attenuation value for different modes at port 1 of the structure at 47GHz is shown below:

Mode Number	Attenuation	Propagation
1	0.12	773.12
2	870.07	0.29
3	870.16	0.2
4	1090.4	0.29

Table 4.1: Gamma values for different modes at port1 at 47GHz frequency for4.1 mm width of dielectric strip.

Now both the height and width of the waveguide used in the transition is matched with the dielectric strip for matching and getting a proper S21 values in the required frequency region. Here a 30×4.78×2.39 mm waveguide is used for matching. The strip dimension is shown below:

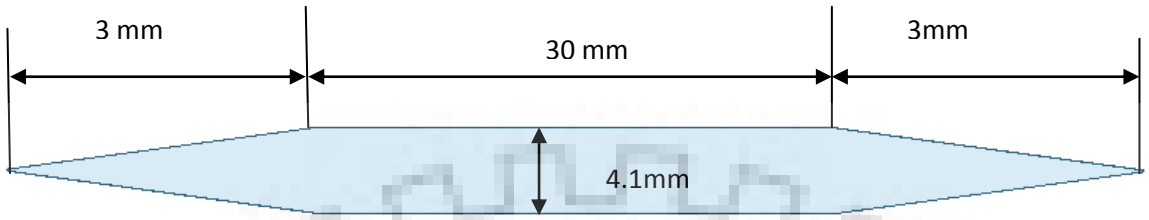

Figure 4.5: Top view of dielectric strip.

The metal plate length is 20 mm and the tapering starts 5mm inside the transition waveguide. The taper width and height at the end is 0.1 mm and 2.35mm respectively. To show the importance of matching of height of the waveguide with the dielectric strip a simulation was done with height of the waveguide as 10 mm instead of 2.39 mm which was nearly equal to the height of the dielectric strip (2.35mm). Instead of allowing a single mode to propagate multiple modes were allowed. The same was observed when there is mismatch of width of the dielectric strip where the breadth was changed from 4.78 mm to 20 mm. The propagation and attenuation value for different modes at port 1 of the structure at 47GHz is shown below:

Mode Number	Attenuation	Propagation
1	0.036	933.64
2	0.0566	778.06
3	0.0533	768.67
4	0.087	711.81

Table 4.2: Gamma values for different modes at port1 at 47GHz frequency for height 10mm of the waveguide

Mode Number	Attenuation	Propagation
1	0.06	972.51
2	0.07	933.67
3	0.07	865.09
4	0.09	758.73

Table 4.3: Gamma values for different modes at port1 at 47GHz frequency for width 20mm of the waveguide

Generally the S21 values for NRD transitions are observed to be around 1 dB for waveguide transitions where a material having low loss tangent value like teflon is used as a dielectric medium. But in the above simulations the S21 values hover between 3-5 dB. Teflon has low dielectric loss tangent of 0.004 whixh can be the main reason for high S21. So this low S21 value is due to the high loss tangent value of PLA (0.008). Now for low loss tangent value the S21 value will drastically improve. The effect of loss tangent on S21 is depicted in figure 4.6.

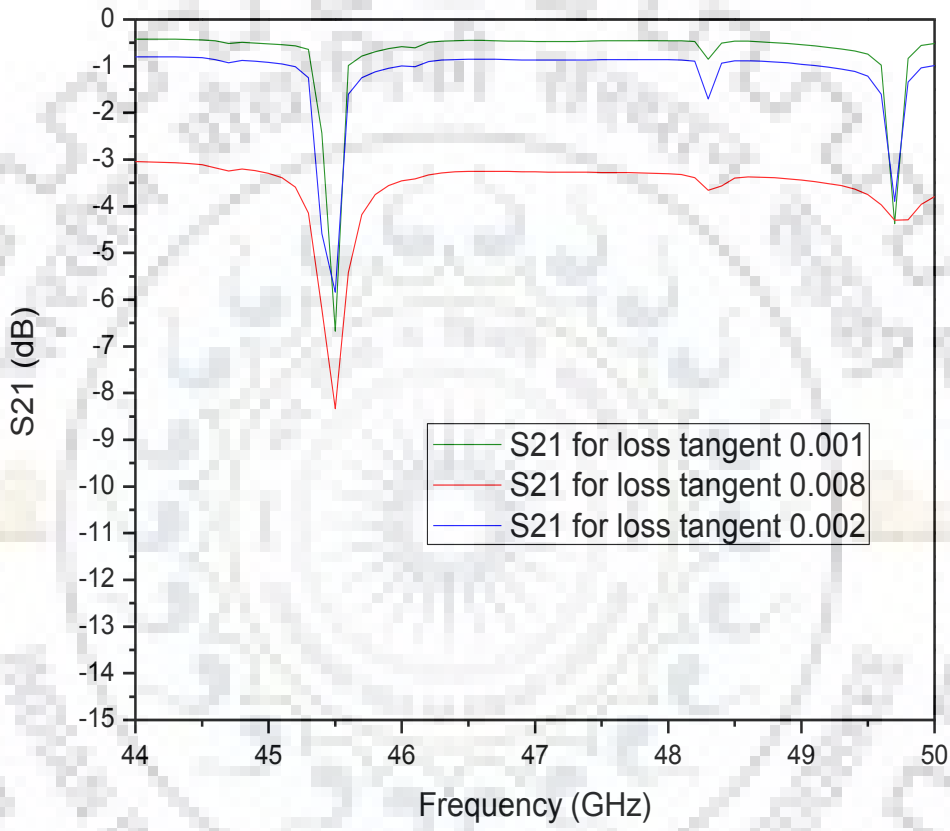

Figure 4.6: S21 plot with variation of loss tangent

So the above plot proves that the design works properly and low S21 value is due to the high loss tangent of PLA.

4.2 Simulation and analysis of Bandpass filter with NRD to Waveguide transition

A Single element and a 3 element bandpass filter having a structure similar to that of a step impedance resonator is designed with centre frequency 47GHz. Main purpose of simulation of this structure is to check whether hybrid technology configuration such as bandpass filter can be realized using this transition. A simple Single element bandpass filter is proposed whose simulation setup is and the top view of the dielectric strip is depicted in figure 4.7 and 4.8. .

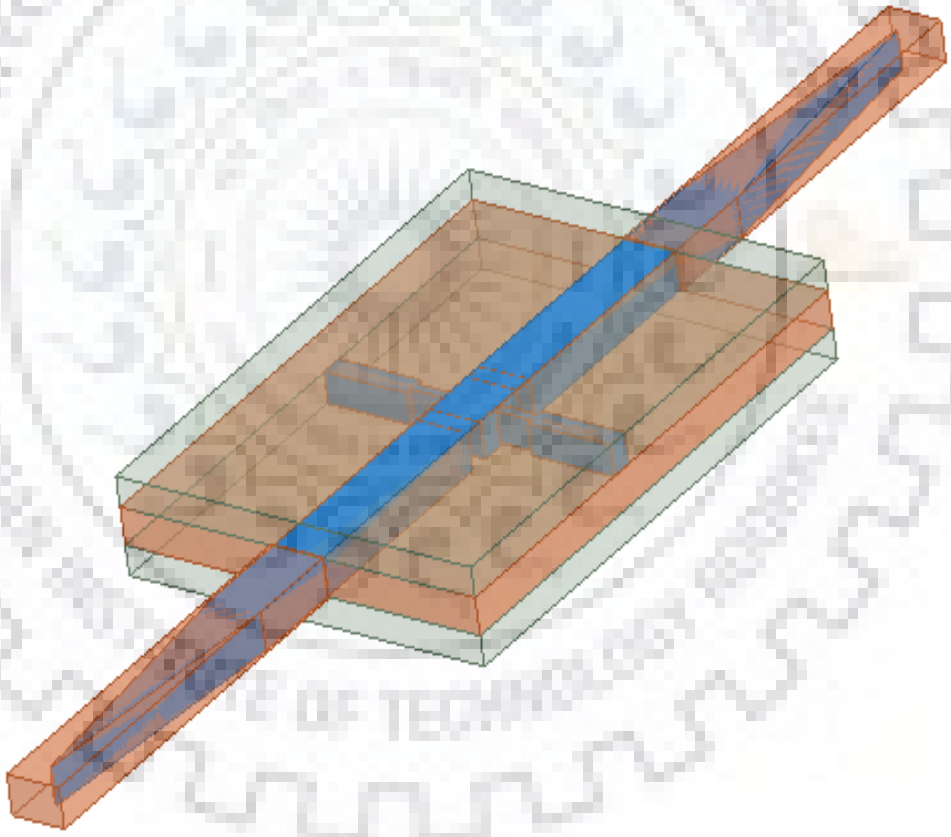

Figure 4.7: Simulation setup for Single element filter.

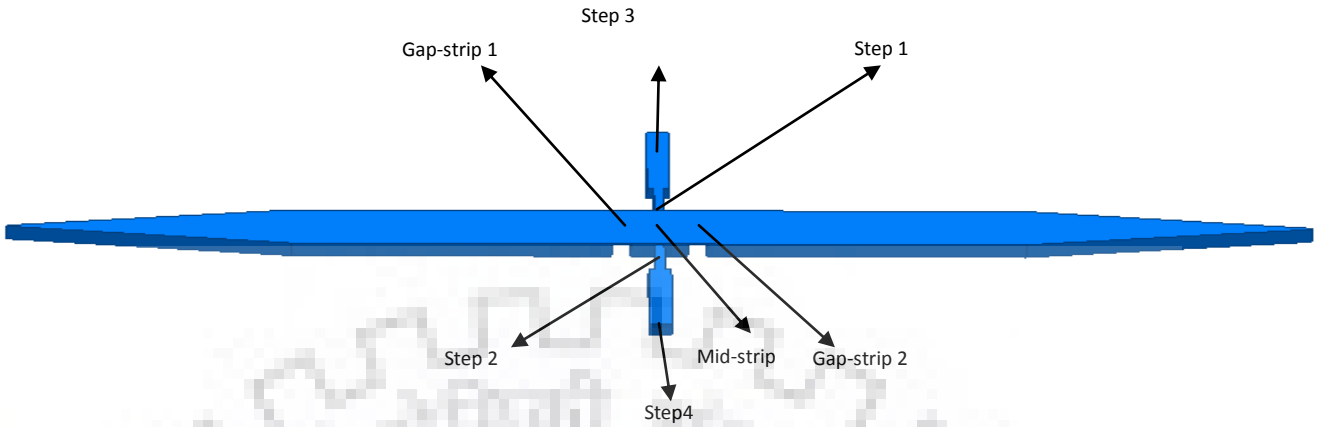

Figure 4.8: Top view of dielectric strip of Single element filter.

Structure name	X-dimension (mm)	Y-dimension (mm)	Z-dimension (mm)
Step 1,Step 2	0.7	3	2.1 (0.2 mm above lower metal plate)
Step 3,Step 4	1.66	7	2.1 (0.2 mm above lower metal plate)
Gap-strip 1, Gap-strip 2	1.4	4.2	0.1
Mid strip	4.2	4.2	2.5

Table 4.3: Dimension of the Single element bandpass filter

Here just like the waveguide to NRD transition a tapered dielectric strip is used. The end width and end height of the tapered structure is 0.1 mm and 2.5 mm respectively. The length of the tapered section is 21 mm and it starts from 7mm inside the waveguide and the length of the strip inside NRD is 40mm. The dimension of the non-tapered portion is 54×4.2×2.5 mm. The S11 and S22 plot of the proposed filter is shown below:

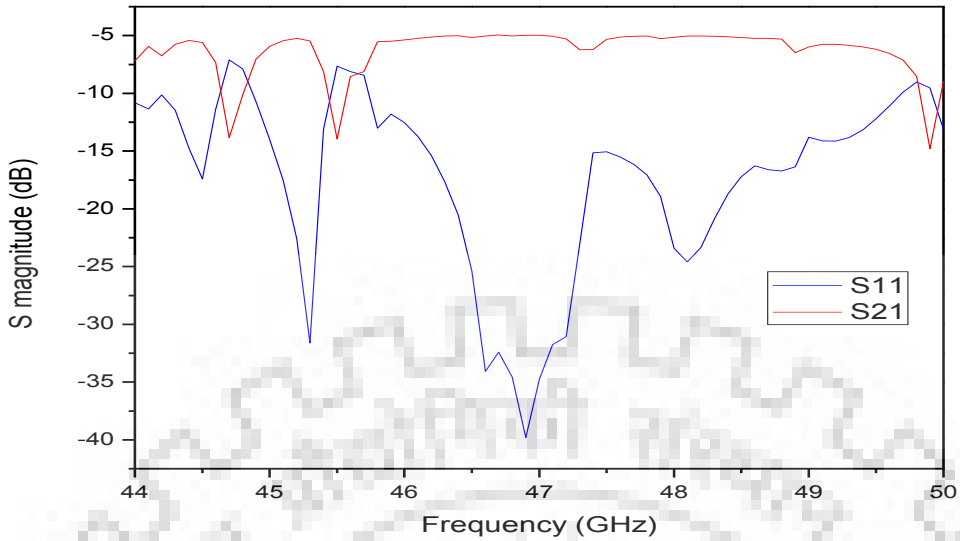

Fig 4.9: S11 and S21 plot for frequencies 44-50 GHz of the Single element filter.

In figure 4.9 the centre frequency of the filter is 46.9 GHz which is close to 47GHz. S11 and S22 at 46.9 GHz is -39.7928 dB and -4.96 dB. The passband of the filter is quite poor and requires further improvement. So a 3 element filter is designed. The simulation setup is similar to that of the Single element bandpass filter. The top view of the dielectric strip and its dimensional analysis is depicted below.

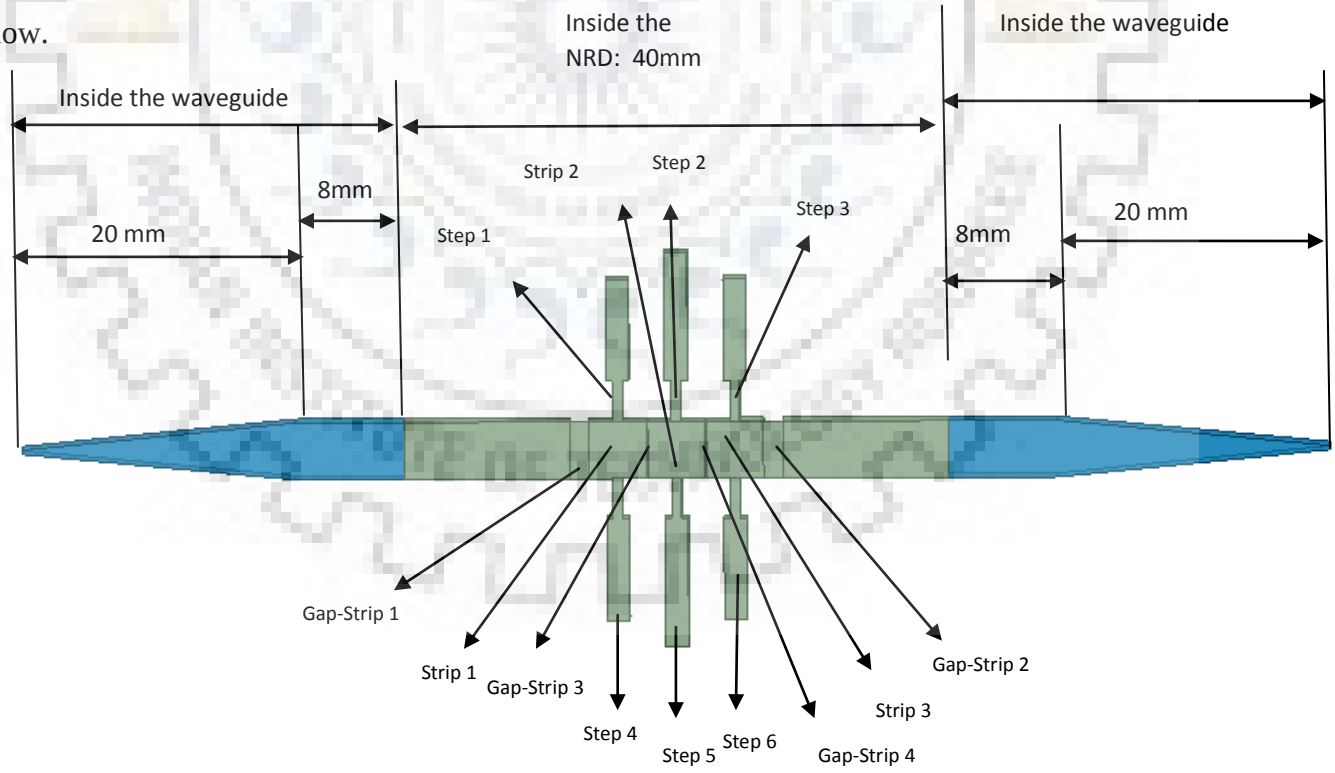

Figure 4.10: Top view of dielectric strip of 3 element filter.

Structure name	X-dimension (mm)	Y-dimension (mm)	Z-dimension (mm)
Step 1, Step 2, Step 3	0.7	3	2.1 (0.2 mm above lower metal plate)
Step 5	1.66	9.5	2.1 (0.2 mm above lower metal plate)
Step 4, Step 6	1.66	7.5	2.1 (0.2 mm above lower metal plate)
Gap-strip 1, Gap-strip 2	0.1	4.2	0.1
Gap-strip 1, Gap-strip 2	1.4	4.2	0.1
Strip 1, Strip 2, Strip 3	4.2	4.2	2.5

Table 4.4: Dimension of the 3 element bandpass filter

The end width and end height of the tapered structure is 0.1 mm and 2.5 mm respectively. The S11 plot and S21 plot for the 3 element filter is shown in figure 4.11.

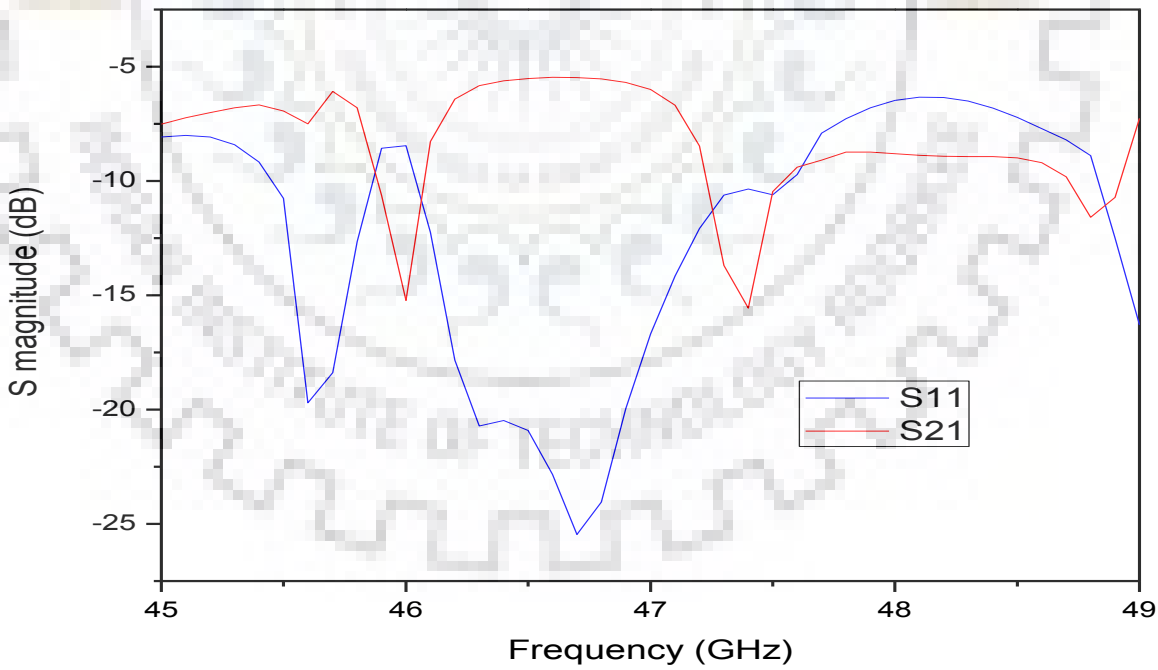

Fig 4.11: S11 and S21 plot for frequencies 45-49 GHz of the 3 element filter.

The centre frequency of the filter is 46.7 GHz which is quite close to 47 GHz which was our target centre frequency. The S11 and S21 at the centre 46.7 GHz is -25.464 dB and 5.47 dB respectively. The passband of the filter has improved considerably as S21 values dip to -15 dB and -16 dB at 46GHz and 47.4 GHz. The bandwidth obtained is 1.4 GHz in this structure.

4.3 Simulation and analysis of Bandstop filter with NRD to Waveguide transition

A bandstop filter with centre at 47GHz is designed using spurline element. The length is equal to one-fourth the guided wavelength ($\lambda_g/4$) which for 47 GHz is equal to 0.97 mm. The top view of the spurline structure is shown below:

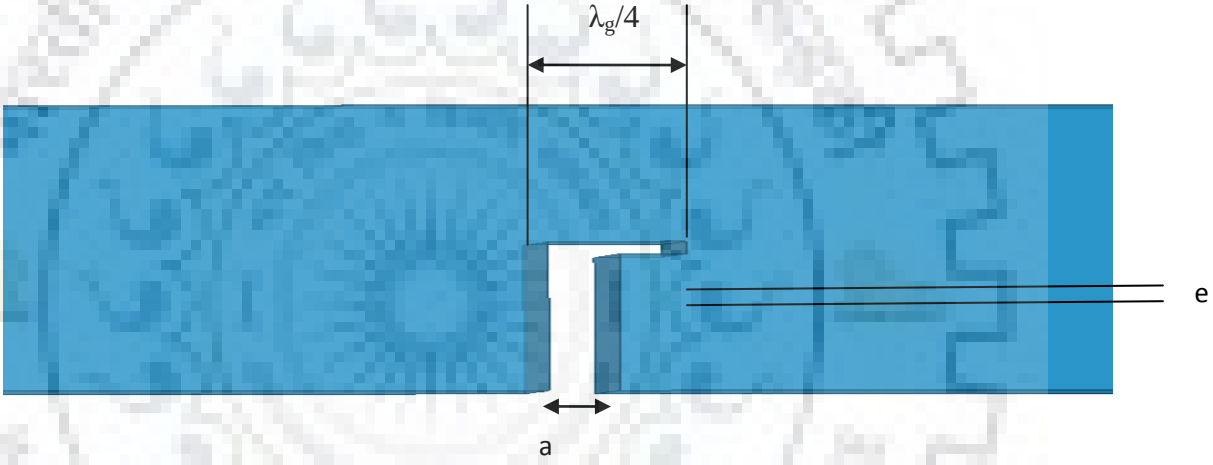

Figure 4.12: Top view of Spurline element.

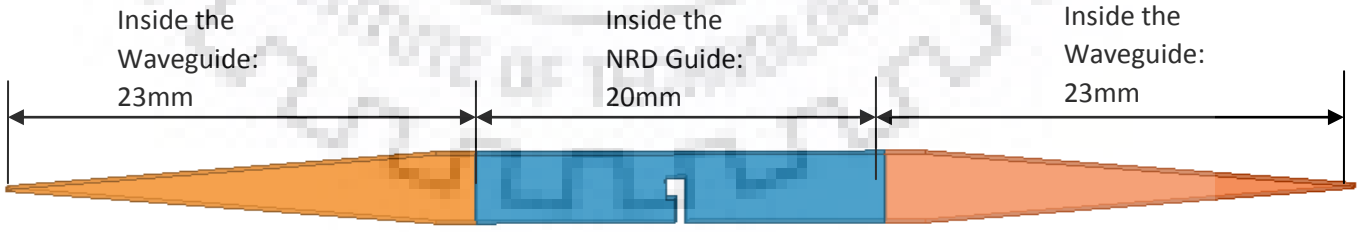

Figure 4.13: Top view of Dielectric strip.

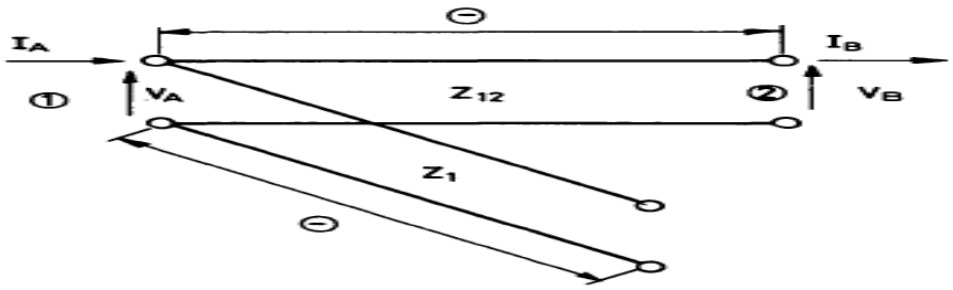

Figure 4.14: Equivalent circuit of spurline section.

The height and width at the end of the taper is 2.5mm and 0.1 mm respectively. Variation of the breadth of the dielectric strip was simulated as shown in fig: 4.13 with height fixed at 2.5mm, b fixed at 0.5mm and e fixed at 1.2mm respectively.

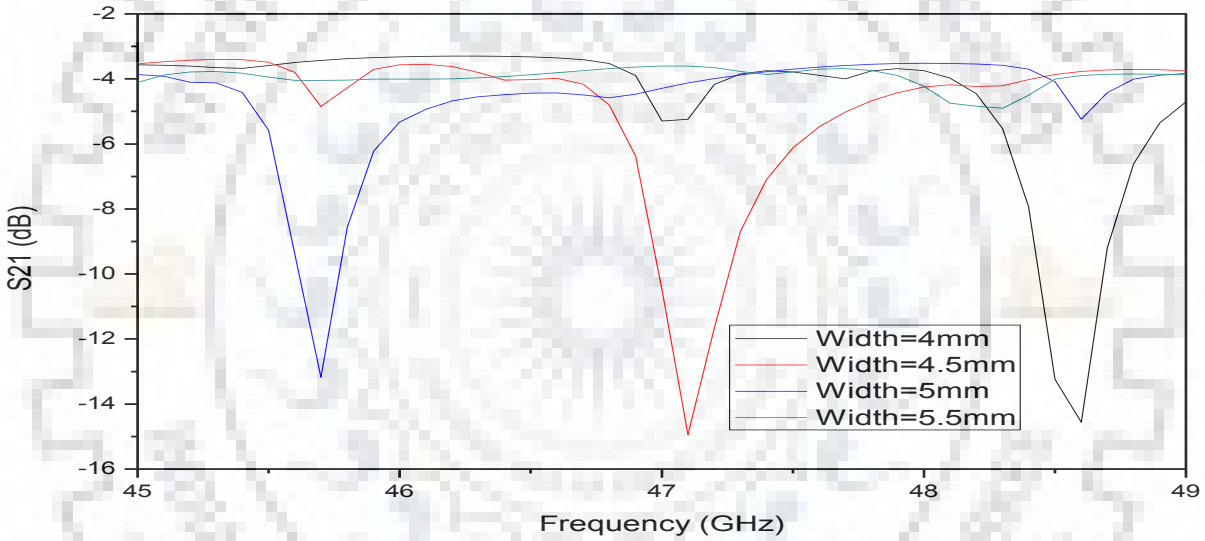

Figure 4.15: S21 plot for variation of the breadth of the dielectric strip

From the figure 4.13 it is evident that varying the breadth of the dielectric strip shifts the centre frequency of the bandstop filter. The width of the dielectric strip is fixed at 4.5mm based on the result obtained from figure 4.13. To optimize further variation of a and e is done.

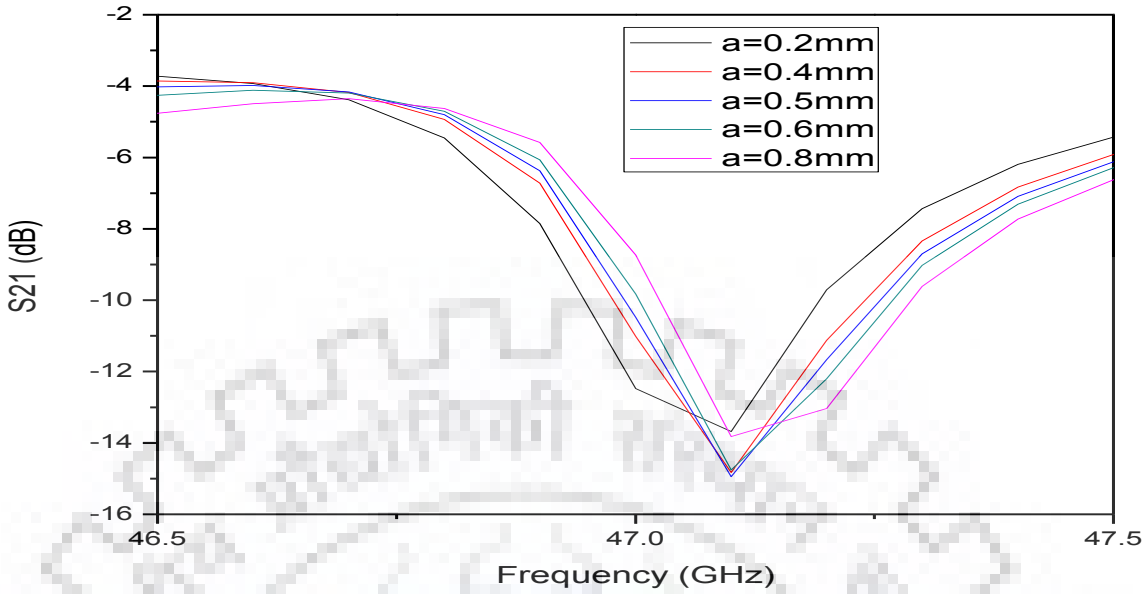

Figure 4.16: S21 plot for variation of a

Based on the result obtained from the above fig 4.15 a is fixed at 0.5mm.

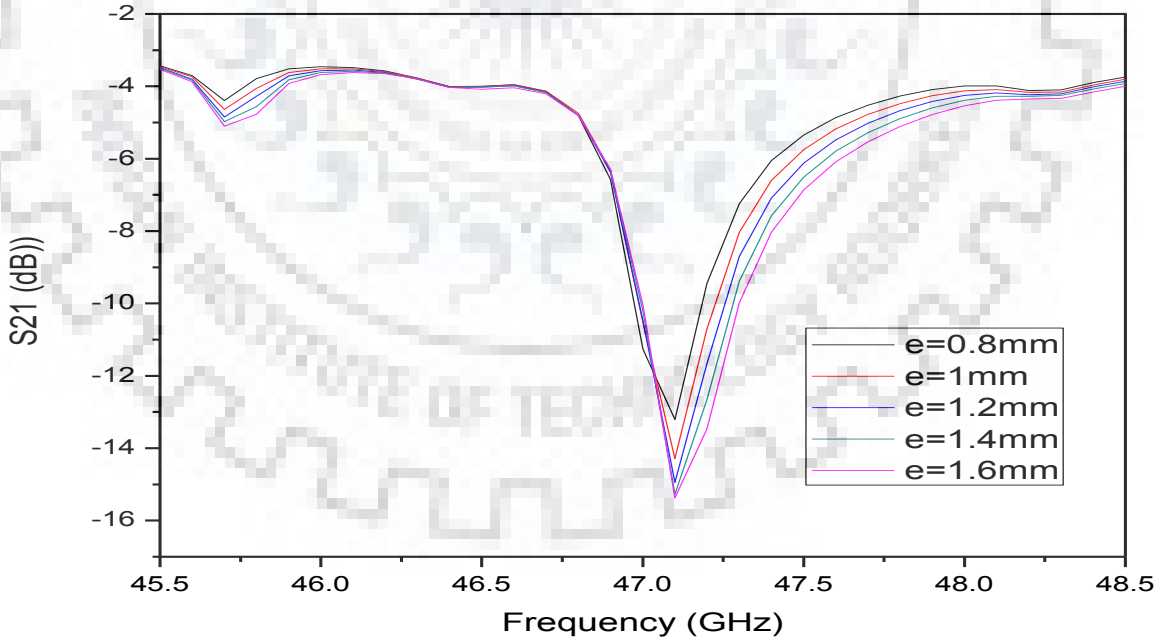

Figure 4.17: S21 plot for variation of e

Based on the results obtained e is fixed at 1.2mm. The final structure consists of a dielectric strip of width 4.5mm, a = 0.5mm, e =1.2 mm. The S21 plot after optimization is given below.

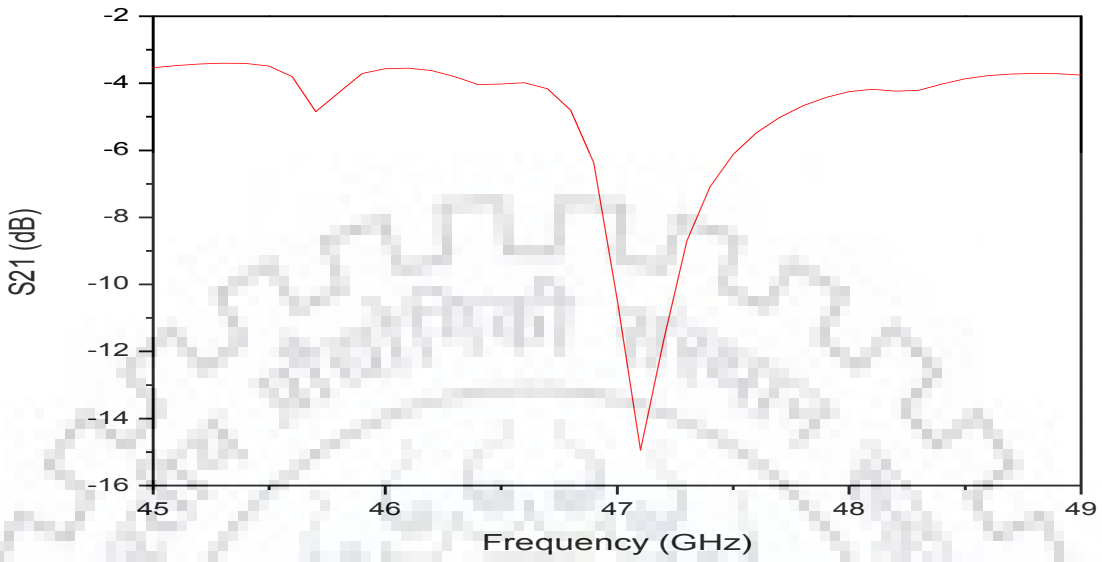

Figure 4.18: S21 plot for bandstop filter

The centre frequency is obtained at 47.1 GHz which is near to the target centre frequency 47 GHz. The S21 value at centre frequency is -14.942 dB.

4.4 Conclusion

In this chapter NRD to waveguide transition was designed which showed promising result for the frequency range 44-50 GHz. After optimization S21 was seen to be around 3.5 dB with its worst value being 8.3 dB at 45.5 GHz frequency. The low value of S21 was assumed to be due to the high loss tangent value of PLA which was used as a dielectric medium in the guided structure. The effect of loss tangent on S21 showed in figure 4.6 proves that our assumption was correct. A Single element and a 3 element bandpass filter with centre frequency 47GHz was designed and simulation results were promising. The 3 element filter depicted good passband characteristics. The final structure had centre frequency 46.7 GHz. Then a bandstop filter was designed with centre frequency 47.1 GHz using a spurline structure. Even though the results were promising one major flaw in this waveguide transition is that it allows parasitic mode to propagate through it.

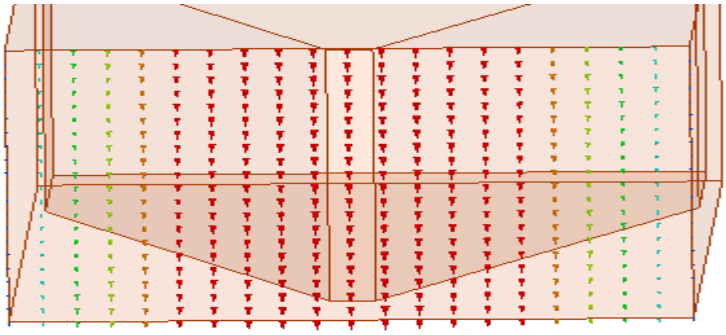

Fig 4.19: E field lines at port 1.

The mode allowed by the guided structure consists of E field lines perpendicular to the dielectric strip as shown in figure 4.18. So further NRD based circuits were not done with this transition. Poor matching and transmission characteristics were observed when the E field of 1st mode of the NRD guide was parallel to the dielectric strip.To solve this issue a waveguide transition with horn antenna can be used which will be discussed in the next chapter.

Chapter 5: Simulation and Analysis of NRD to Waveguide Transition using Horn Antenna

5.1 NRD to Waveguide transition using Horn Antenna

As reported by T. Yoneyama in [21] a customised horn was used where the H-plane is tapered and E-plane is flared. A tapered dielectric strip is inserted in the transition part just like in the waveguide transition. Here the tapered length was fixed at 3 times the free space wavelength. Here the length of the flared part of the horn antenna was fixed at 3 times the free space wavelength. Here the matching of height of the flared part of the horn antenna with the height of the dielectric strip of the NRD guide is of utmost importance for proper matching. The matching of the breadth of the tapered dielectric with that of the width of the waveguide is also important for obtaining proper result. Here the height and breadth is fixed at 2.39mm and 4.78 mm respectively in simulation. The length and breadth is same as that of the WR22 waveguide which is a standard rectangular waveguide. The simulation setup of the transition structure is given below:

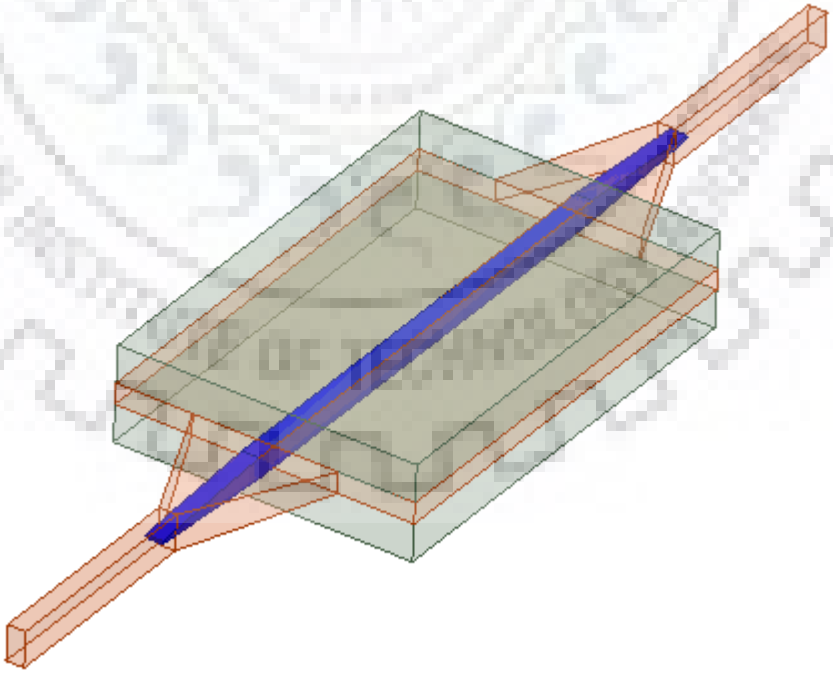

Fig 5.1: Simulation setup of the transition structure

Simulations were done for frequency range 44.5 GHz to 49.5 GHz with main focus around 47 GHz. The main objective of the transition structure is to have low S11 values and S21 values for the entire frequency region. Simulations were done in HFSS 17.1. The S11 and S21 plot for variation of breadth of the dielectric strip made up of PLA where height is fixed at 2.8mm is shown below:

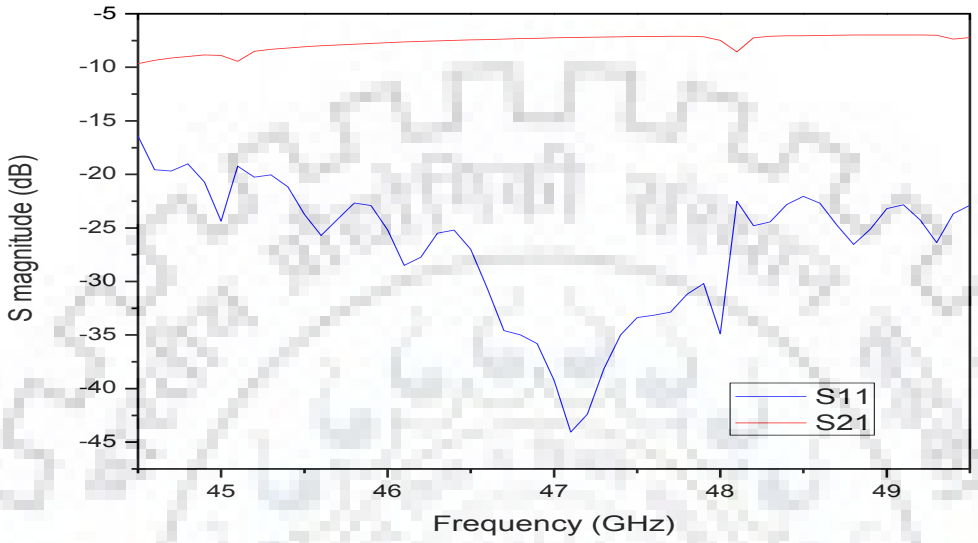

Fig 5.2: S11 and S21 plot for frequencies 44.5-49.5 GHz of NRD to horn transition for 2.2mm width of dielectric strip.

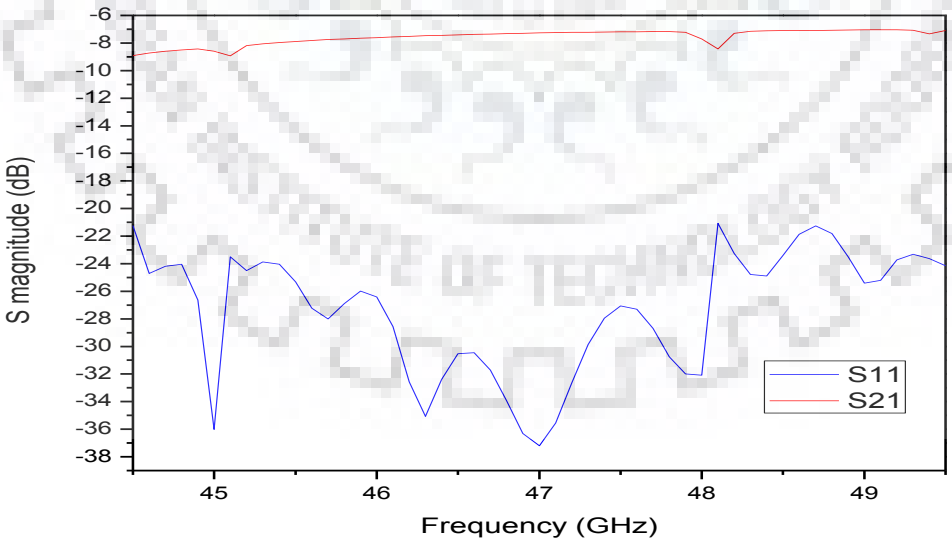

Fig 5.3: S11 and S21 plot for frequencies 44.5-49.5 GHz of NRD to horn transition for 2.3mm width of dielectric strip.

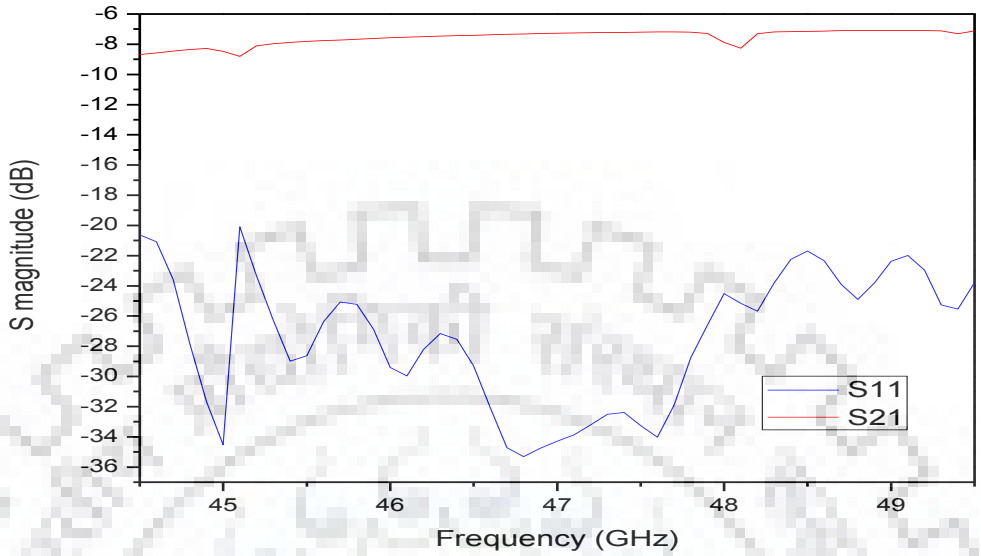

Fig 5.4: S11 and S21 plot for frequencies 44.5-49.5 GHz of NRD to horn transition for 2.35mm width of dielectric strip.

From the above plots dielectric strip breadth of 2.3mm shows good matching and transmission characteristics of the transition structure as the S11 remains less than -21 dB and S21 remains mostly at 7dB throughout the frequency range. So the breadth of the strip is taken as 2.3mm. The dip in S21 at certain frequencies is due to discontinuity in the transition structure. This transition structure allows a single mode to propagate. The propagation and attenuation value for different modes at port 1 of the structure at 47GHz is shown below:

Mode Number	**Attenuation**	**Propagation**
1	0.121	773.85
2	870.08	0.29
3	870.21	0.197

Table 5.1: Gamma values for different modes at port1 at 47GHz frequency for 2.3mm width of dielectric strip.

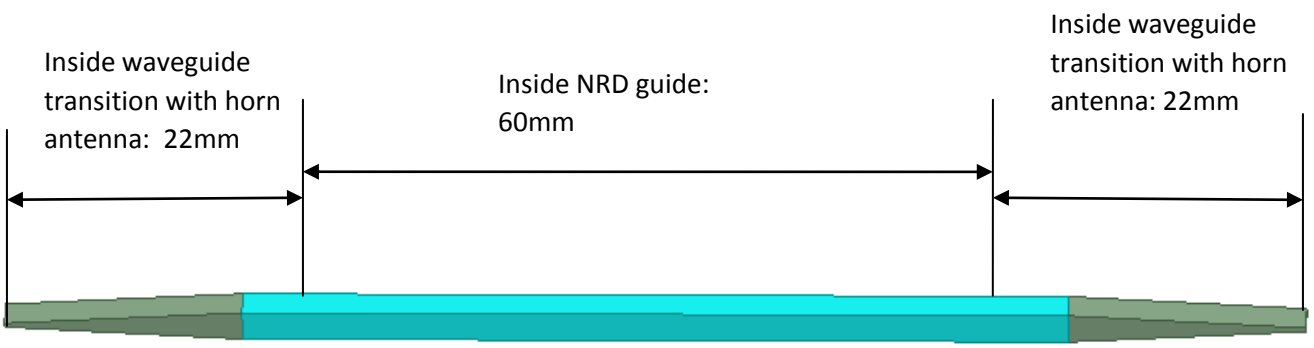

Fig 5.5: Side view of the dielectric strip

The tapering of the dielectric starts 3mm into the horn antenna and the tapered length is 19.5mm. The end-width and height of the tapered structure is 2.3mm and 0.4 mm respectively. The length of the tapered structure is 19.5mm. The dimension of the transition structure is given below:

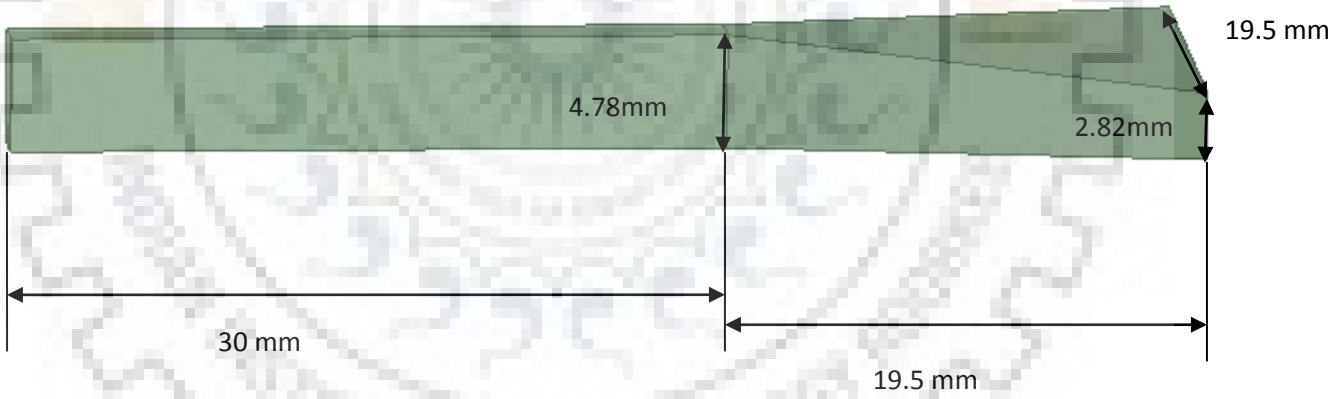

Fig 5.6: Side view of the transition structure

The breadth of the rectangular waveguide is 2.39 mm. Generally the S21 values for NRD transitions are observed to be around 1 dB for waveguide transitions where a material having low loss tangent value like teflon is used as a dielectric medium. But in the above simulations the S21 values hover between 7-9 dB. The low S21 value is due to the high loss tangent value of PLA (0.008). Now for low loss tangent value the S21 value will drastically improve. The effect of loss tangent on S21 is depicted in figure 5.7 which proves that our assumption is correct.

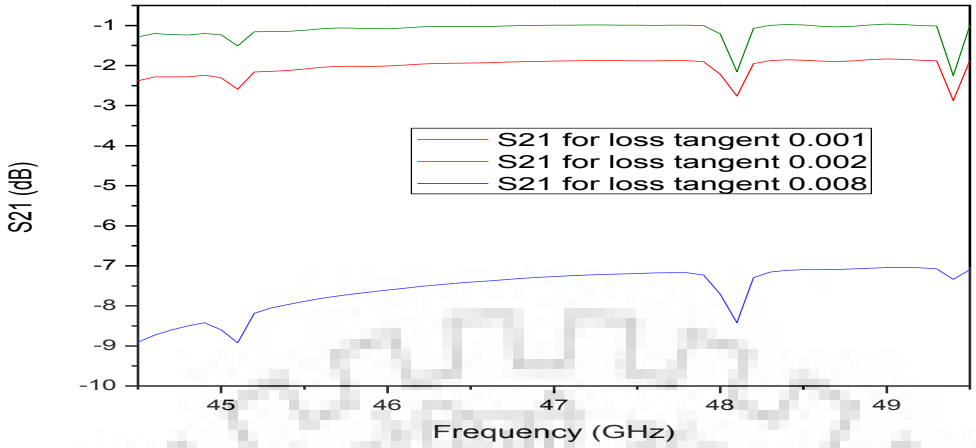

Fig 5.7: S21 plot with variation of loss tangent

5.2 Conclusion

In this chapter NRD to waveguide transition with horn antenna was designed which showed promising result for the frequency range 44.5-49.5 GHz. After optimization S21 was seen to be around 7 dB with its worst value being 9 dB. The low value of S21 was assumed to be due to the high loss tangent of PLA which was used as a dielectric medium in the guided structure. The effect of loss tangent on S21 showed in figure 5.7 that our assumption was correct. In this transition only a single mode is allowed to propagate and the E field lines of that mode is parallel to the dielectric strip which is the field line of the desired mode (LSM 11).

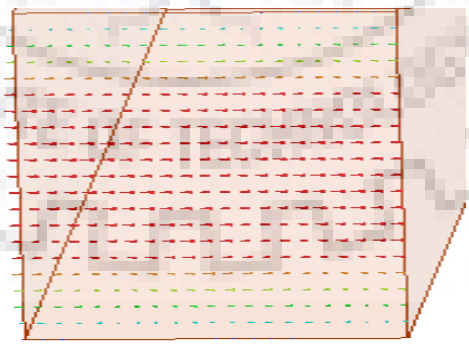

Fig 5.8: E field lines at port 1.

Chapter 6: Simulation, Analysis and Measurement of NRD to Microstrip Transition

6.1 NRD to Microstrip Transition

In this chapter NRD to Micro-strip transition has been designed, simulated and realized practically. In this transition both the dielectric strip and micro-strip line have a common ground plane [25]. For coupling the slots are made on the ground plane. The slots are at an angle 90° with the micro-strip line and parallel to the dielectric strip while the microstrip lines are at an angle 90° with the dielectric strip for single mode operation. The simulation setup is shown below:

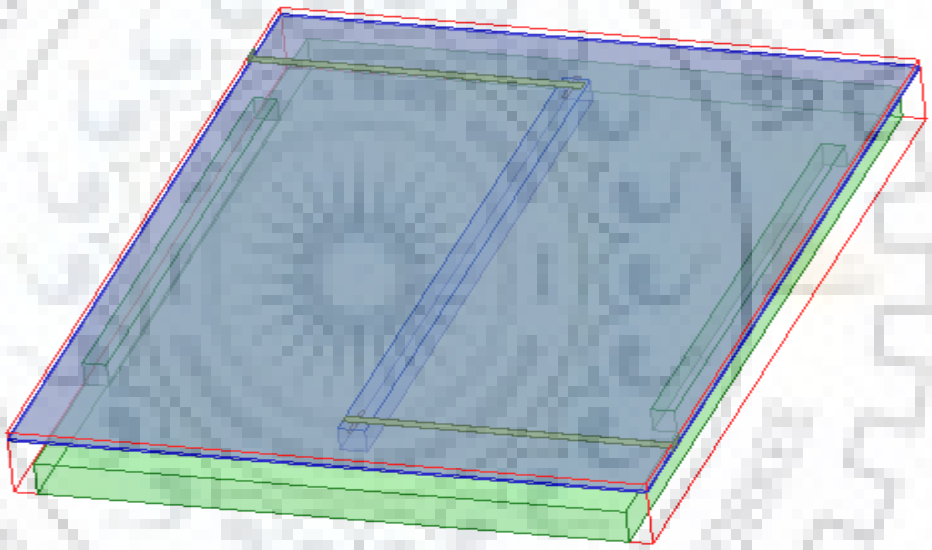

Fig 6.1: Simulation setup of the transition structure

In the simulation Rogers/RT duroid 5800 (ε_r=2.2) is used as substrate which has a height of 0.254mm. The region above the microstrip line should be air, so for that an air region is taken which encompasses the entire transition structure. As mentioned in L. Han, et al in [12], the performance of the transition is mainly dependant on the open end of the microstrip line and slot. The separation between the microstrip line is fixed at 63mm, microstrip line width is 1mm, substrate dimension is 80×54×0.254 mm, the lower metal plate dimension is 80×50×4 mm, the dielectric strip dimension is 66×2.3×2.8 mm, the dimension of ground plane made up of copper is 80×54×0.018 mm. A

50×2×2.8 mm metal channel is used to hold the substrate. The simulations are done using HFSS 17.1 for frequency ranges 46.4 to 47.6 GHz with main focus at 47GHz.

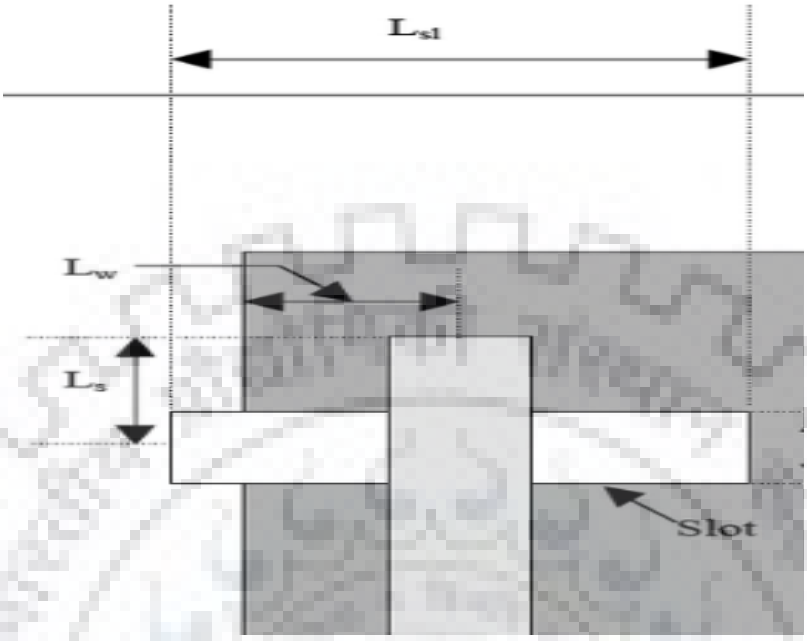

Fig 6.2: Top view of microstrip line and slot part of transition

So plot of S21 with variation of the length of open end of microstrip line (ls) is shown below:

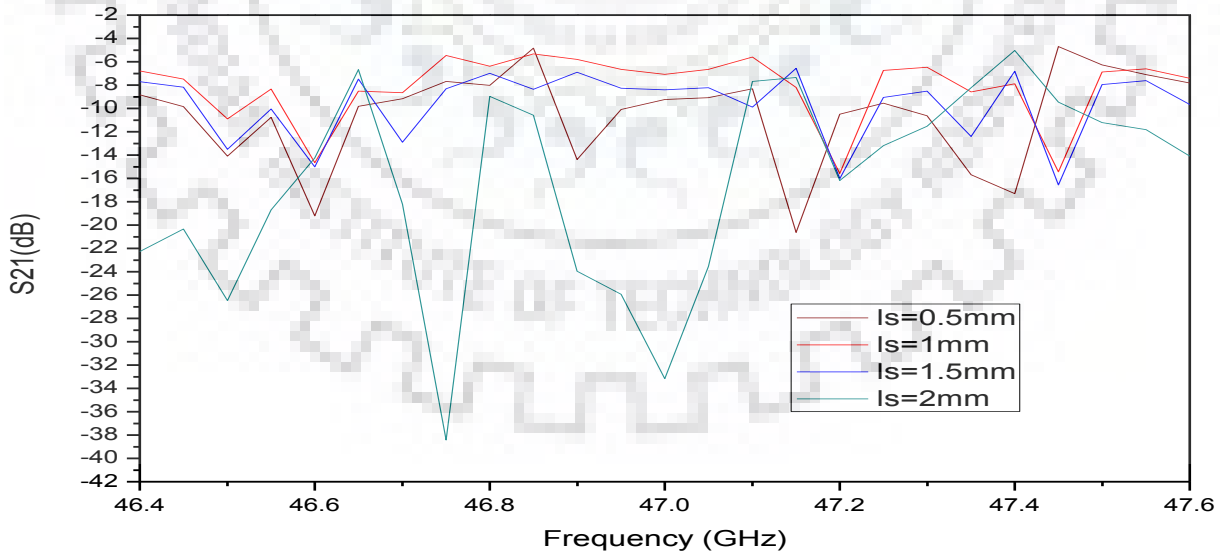

Fig 6.3: S21 plot with variation of length of open end of microstrip line

The length of the open end of the microstrip line is set at 1mm and total length of the microstrip line is 28mm. So plot of S21 with variation of length of open end of the slot is shown below

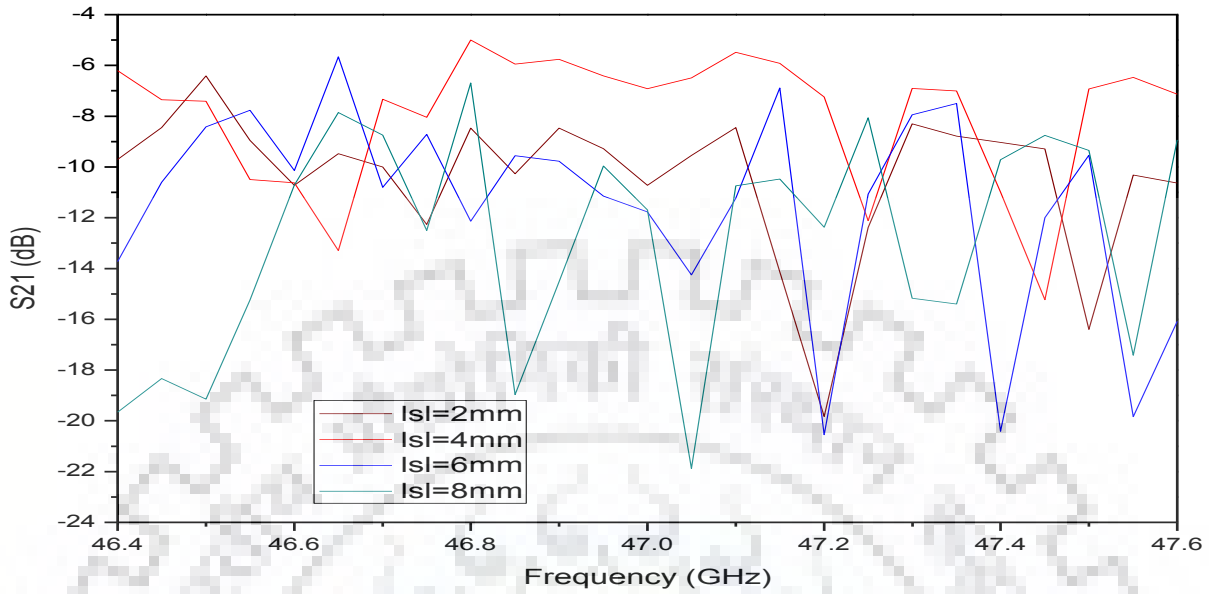

Fig 6.4: S21 plot with variation of length of slot.

The length of the slot is fixed at 4mm based on the results obtained from fig 6.4. The S21 and S11 plot after optimization is given below

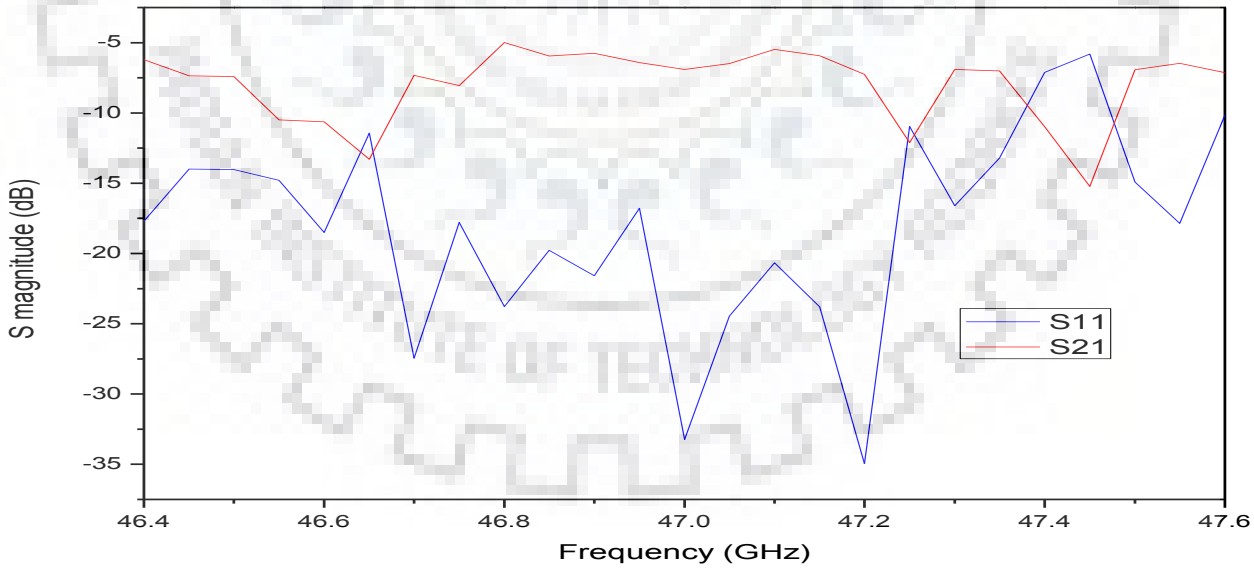

Fig 6.5: S11 and S21 plot for NRD to Microstrip transition

The optimized result shows a bandwidth of 500 MHz where the S21 value does not drop below -10dB and S11 remains less than -15dB. The S21 values are quite low due to high dielectric loss tangent of PLA which is 0.008. For low loss tangent value the S21 will drastically improve. The effect of loss tangent on S21 is depicted in figure 6.6.

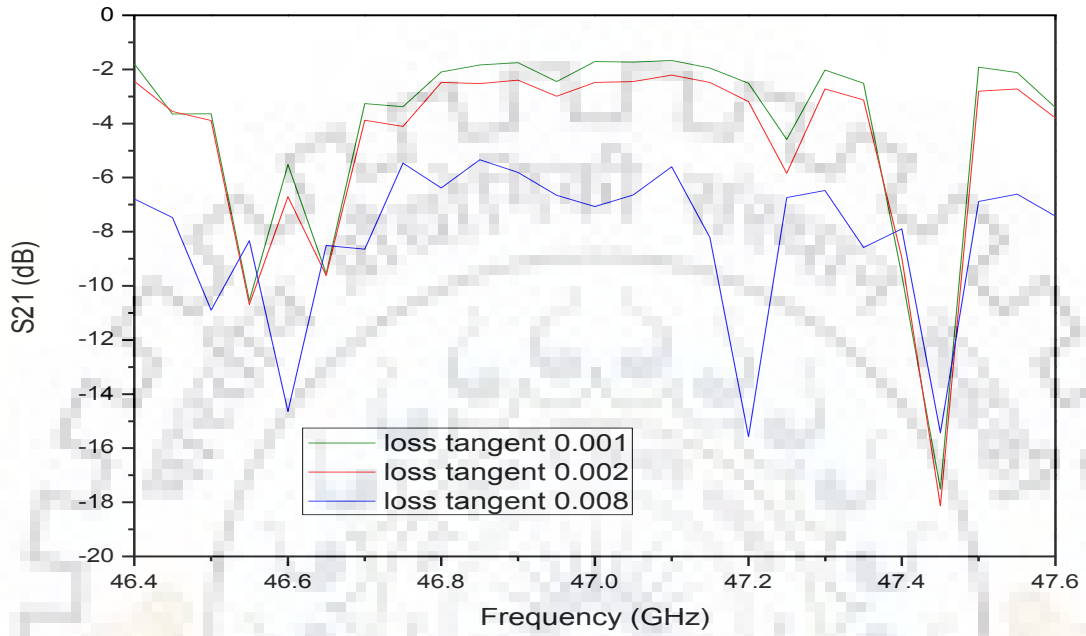

Fig 6.6: S21 plot with variation of loss tangent

S21 plot in Fig 6.6 proves that our assumption is correct. The transition structure allows only a single mode to propagate. The propagation constant at port 1 for frequency 47 GHz is given below:

Mode Number	Attenuation	Propagation
1	1.4782	1347.4
2	1122.7	0.158
3	1604.3	0.385

Table 6.1: Gamma values for different modes at port1 at 47GHz frequency.

6.2 Experimental Setup and Results

The experimental setup is shown below:

Fig6.7 :Top view of substrate with connector

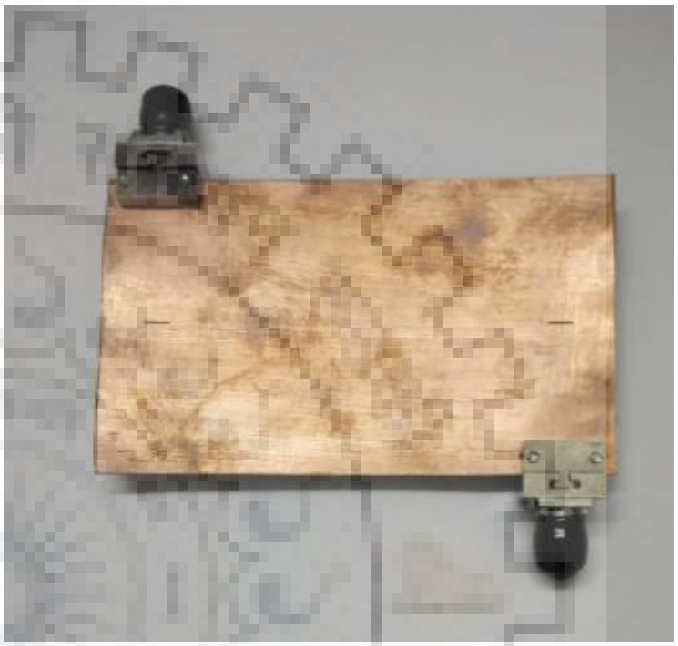

Fig 6.8 :Top view of ground plane with connector and slots

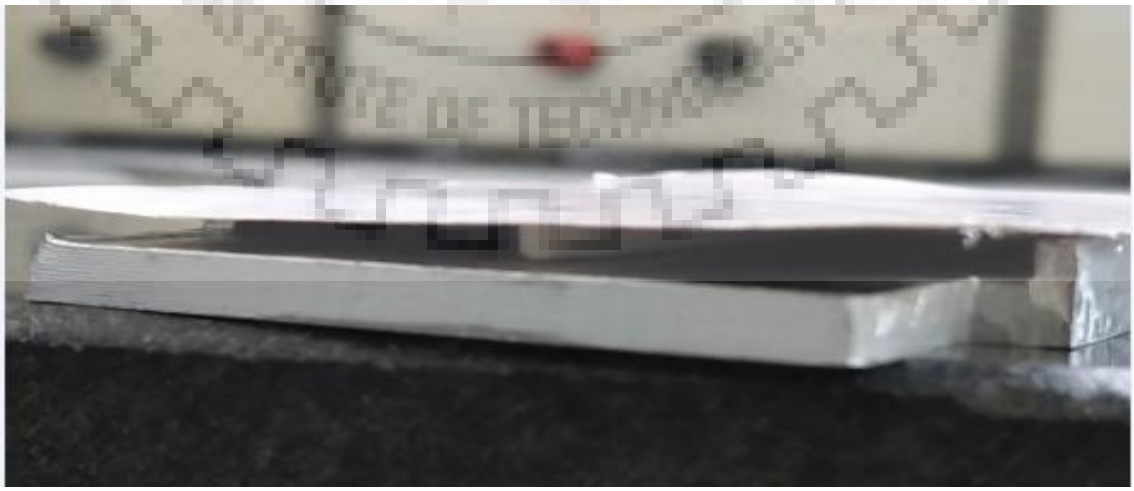

Fig 6.9: Front view of the assembled structure

Aluminium metal plate has been used. The ground plane and microstrip lines are made up of copper. The lower part of the connector which has to be below the substrate has a height of 5 mm while the separation between the ground plane and the metal plate is 2.8mm. The metal plate had to be cut so that the connector can be accommodated for obtaining result in the vector network analyzer. The dielectric strip made up of PLA was printed in Ultimaker extended 2+ using a 0.6mm nozzle with minimum resolution 50 micron. The substrate was made by photo etching. Parts of the dielectric strip were attached to the aluminium base plate by an adhesive so that the slots and the strip are properly aligned. The connectors were mounted on the substrate as shown in fig 6.8.

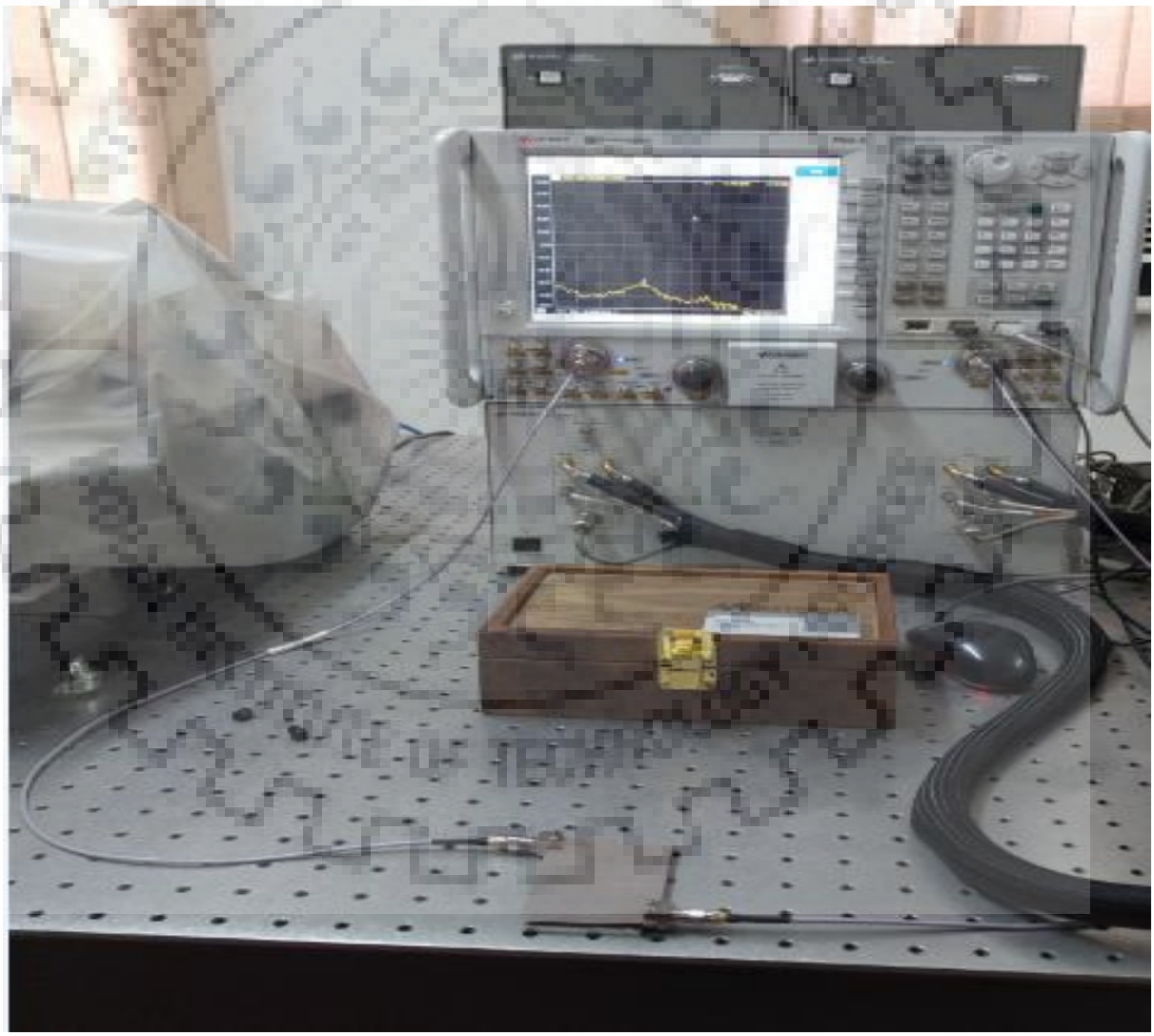

Fig 6.10: Measurement setup

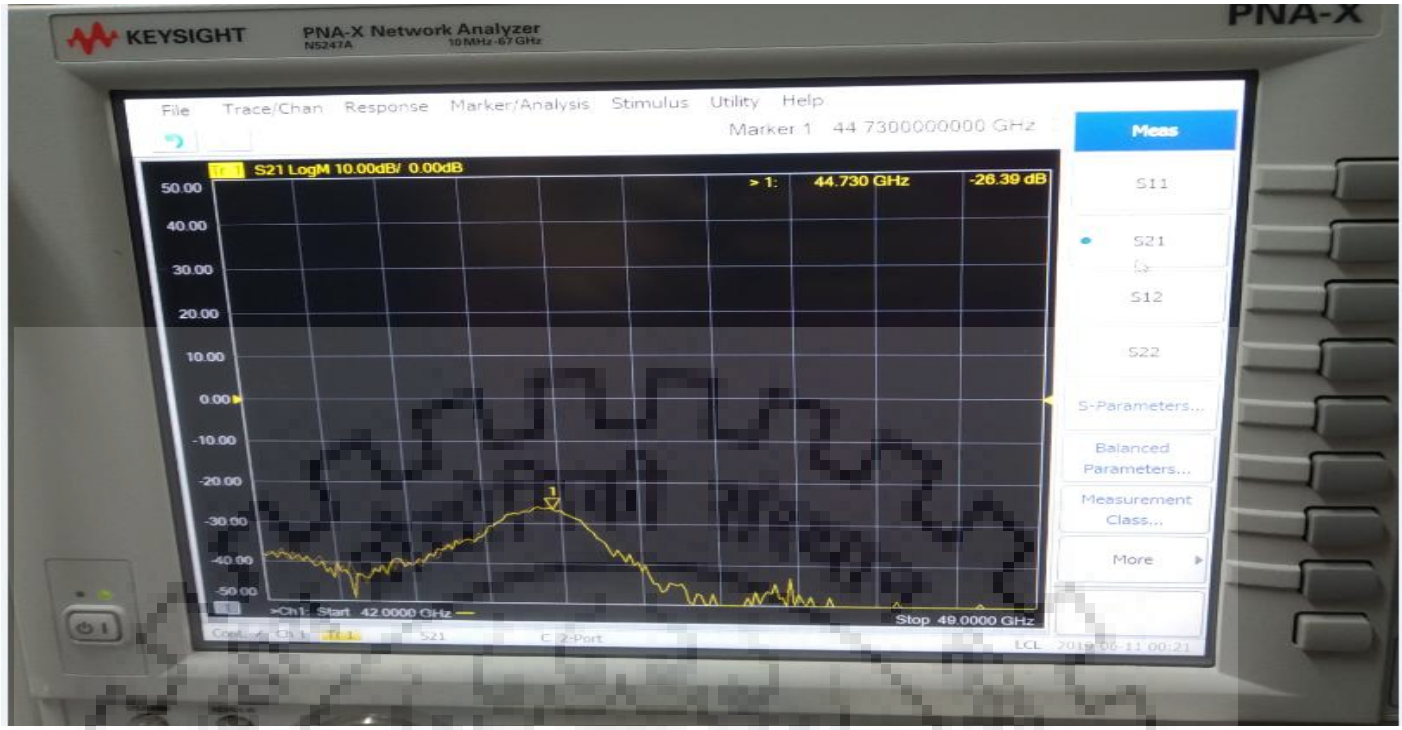

Fig 6.11: Measured S21 plot for frequency range 42-49 GHz

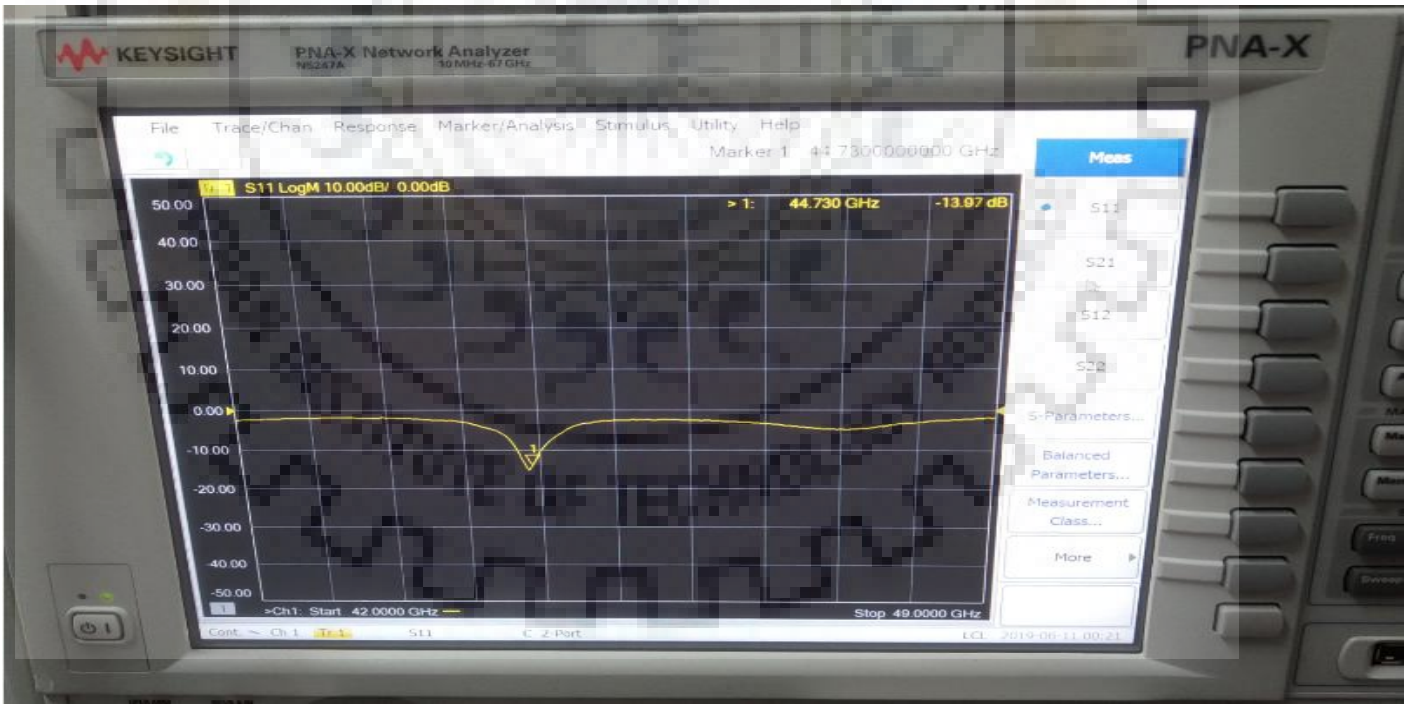

Fig 6.12: Measured S11 plot for frequency range 42-49 GHz

The best S21 and S11 value is -26.2 dB and -13.9 dB at 44.7GHz.

6.3 Conclusion:

In this chapter a NRD to microstrip transition has been done. The simulation results depicted a band of 500 MHz frequency from 46.7 GHz to 47.2 GHz where S21 value is greater than -10dB. The experimental result varies from the simulation result with best S21 and S11 value is -26.2 dB and -13.9 dB at 44.7GHz. The frequency shift is due to the variation of breadth of PLA strip from 2.3mm. The PLA strip is produced by Ultimaker extended 2+ which is a 3D printer. The printed strip has non-uniform breadth and height. Even after keeping the infill density of the printer to 100%, a completely filled solid structure was not fabricated. The baseplate formed at the start of the print embeds a pattern at the base of the printed strip. At such high frequencies even a small change of 0.1 mm in dimension has an adverse effect in experimental and simulation results. The drop in S21 is due to the connector which has its own transmission losses. Moreover, the lower part of the connector which has to be below the substrate has a height of 5 mm while the separation between the ground plane and the metal plate is 2.8mm. Part of the metal plate had to be cut so that the connector can be accommodated for obtaining result in the vector network analyzer. Furthermore, the drop in S21 value can be also attributed to the fact that an adhesive had to be used to fix the PLA strip on the metal plate which was done so that the slots and the dielectric strip are properly aligned. The adhesive could have been avoided if the substrate or the ground plane was thick enough so that the metal plate, the substrate and ground plane could have been connected via screws. Moreover at high frequencies microstrip lines are not ideal for transition structure as it has its own transmission losses. Simulation setup has been made in accordance with the experimental setup.

Fig 6.13: Printed structure

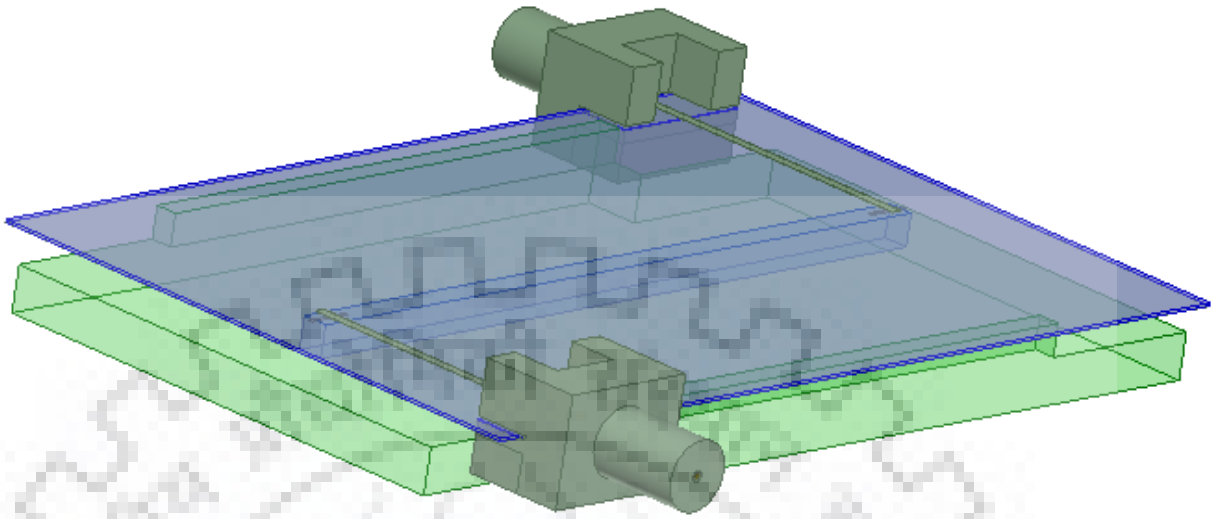

Fig 6.14: Simulation setup of Microstrip to NRD transition with connector

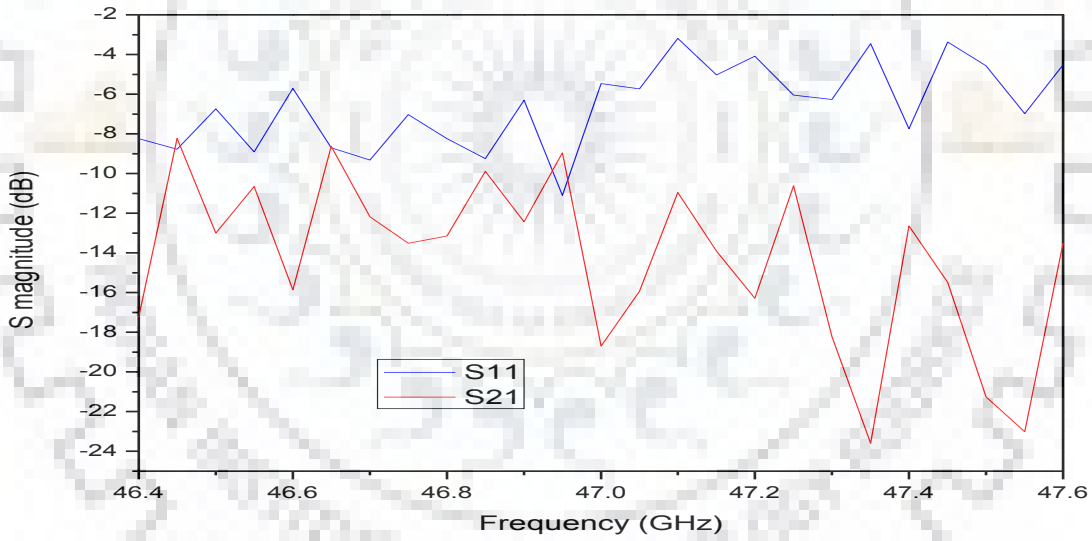

Fig 6.15: S11 and S21 plot for NRD to Microstrip transition

S11 and S21 plot in Fig 6.11 portrays the effect of connector and metal etching as S21 at 47 GHz is reduced to -18.7 dB. So the experimental result is expected to match with the simulation result if all these factors can be taken care of.

Chapter 7: Conclusion and Future Scope

In this dissertation field analysis and propagation constants of different modes of the NRD guide was first analyzed. Then NRD based circuits like bandpass filter were simulated. After getting promising results from the simulation different NRD transitions were analyzed and simulated. All the 3 transitions (waveguide, a waveguide with horn antenna, microstrip transition) showed promising results in simulation. The low S21 values in the transition structures were attributed to high loss tangent value of PLA which was used as a dielectric strip. A bandpass and bandstop filter with centre frequencies 47 GHz were designed with waveguide transition. The idea of using a waveguide transition for realizing different circuits was discarded as it was allowing a single parasitic mode to propagate. To solve this, waveguide transition with horn antenna was used for simulation where the E-plane was flared while the H-plane was tapered. The physical realization of NRD to microstrip transition was made with the main focus on 47 GHz. The experimental results did not match with the simulation results due to various factors such as connector losses, metal etching due to the connector, high transmission losses of microstrip lines at high frequencies, loss due to the discontinuity of coaxial and microstrip line transition, accuracy of the machined components especially non-uniformity of PLA strip, etc . At such high frequencies, even a small change of 0.1 mm in dimension will have an adverse effect in experimental and simulation results One of the major takeaways from this dissertation is that the high loss tangent value of PLA has a major role in the transmission characteristics of the NRD based circuits. Moreover, the 3D printer Ulltimaker extended 2+ used does not produce a smooth structure required for proper experimental analysis of any NRD based circuits. Even after keeping the infill density of the printer to 100%, a completely filled solid structure was not fabricated. This factor was not considered during the simulation of the NRD transition. The future scope could be to realize NRD based circuits using waveguide transition with horn antenna to avoid complications brought on by microstrip transitions. The transition with horn antenna showed promising results in the frequency range 44.5GHz to 49.5 GHz which is important for designing NRD based circuits with centre frequency around 47GHz. Moreover in the future if PLA can be made with a lower loss tangent value can be a viable alternative to Teflon as PLA being biodegradable is not that harmful as Teflon. The biodegradable aspect of PLA can be of paramount importance in the future especially in the day and age of climate change.

References

1. H. H. Meinel, “Commercial applications of millimeter waves: History, present status, and future trends,” *IEEE Trans. Microwave Theory Tech*., vol. 43, pp. 1639–1653, July 1995.
2. K. Wu and L. Han, “Hybrid integration technology of planar circuits and NRD-guide for cost-effective microwave and millimete-wave applications,” *IEEE Trans. Microw. Theory Tech*., vol. 45, no. 6, pp. 946–954, Jun. 1997
3. D. Schrader, “Microstrip circuit analysis”, Upper Saddle River, New Jersey: *Prentice Hall,* 1995.
4. J.-F. Luy, K. M. Strohm, H.-E. Sasse, A. Schuppen, J. Buechler, M. ¨ Wollitzer, A. Gruhle, F. Sch¨affler, U. Guettich, and A. Klaaßen, “Si/SiGe MMIC’s,” *IEEE Trans. Microwave Theory Tech.*, vol. 43, pp. 705–714, Apr. 1995
5. T. Rozzi and M. Mongiardo. “Open electromagnetic waveguides.” *The Institution of Electrical Engineers, Herfordshire*, United Kingdom, 1997.
6. S. K. Koul. “Millimeter wave and optical dielectric integrated guides and circuits.” *John Wiley & Sons*, New York, 1997.
7. T. Yoneyama, "Millimeter research activities in Japan," ibid., pp.3-6, July 1997
8. L. L. Xiao, L. Zhu, and W. X. Zhang, “Analysis of the mono-groove NRD waveguide and antenna,” *Int. J. Infrared Millim. Waves*, vol. 10, pp. 361–370, 1989.
9. T. Yoneyama and S. Nishida, “Nonradiative dielectric waveguide for millimeter wave integrated circuits”, *IEEE Trans. Microwave Theory Tech*., vol. 29, pp.1188-1192, Nov. 1981.
10. N. P. Pathak, “Integration of NRD Guide and Slot line for Millimeter Wave Indoor Wireless Applications”, *Proceedings of WFMN07,* Chemnitz, Germany, 2007.
11. F. J. Tischer “H Guide with Laminated Dielectric Slab,” *IEEE Trans. Microwave Theory Tech*., Vol. MTT-18, pp. 9-15, Jan 1970.
12. L. Han, K. Wu, and R. Bosisio, “An integrated transition of microstrip to nonradiative dielectric waveguide for microwave and millimeter-wave circuits,” *IEEE Trans. Microwave Theory Tech*., vol. 44, pp. 1091–1096, July 1996.

13. R. M. Knox, “Integrated circuits for the millimeter through optical frequency range,” *Proc. of Symposium on Submiilimeter Waves*, Polytechnic Institute of Brooklyn pp. 497–5 16, 1970.
14. J. E. Kietzer, A. R. Kaurs, and B. J. Levin, “A V-Band communication transmitter and receiver system using dielectric waveguide integrated circuits: *IEEE Trans. Microwave Theory Tech*., vol. MTT-24, pp. 297-803, Nov. 1976.
15. F. Kuroki, H. Ohta, and T. Yoneyama, “Transmission Characteristics of NRD Guide as a Transmission Medium in THz Frequency Band” *Joint 30th International Conference on Infrared and Millimeter Waves and 13th International Conference on Terahertz Electronics*, 2005.
16. T. Yoneyama, “Millimeter-wave integrated circuits using nonradiative dielectric waveguide,” *Electron. Commun. Jpn*., vol. 74, no. 2, pp. 20–28, 1991.
17. Y Michael Y. Frankel, Janis A. Valdmains and Gerard A. Mourou, “Terahertz Attenuation and Dispersion Characteristics of Coplanar Transinission Lines”, *IEEE Trans. Microwave theory Tech.*, vo1.39(6), pp.910-916., 1991
18. J.A.G. Malherbe, J.H. Cloete , I.E.Losch, “A Transition to Non-Radiating Dielectric Waveguide,” *IEEE MTT-S International Microwave Symposium Digest*, 1984.
19. S. Mbe Emane, O. Lafond , M. Himdi, “Nonradiative dielectric (NRD) waveguide to rectangular waveguide transition in millimetre waves,” *11th International Symposium on Antenna Technology and Applied Electromagnetics* , 2017.
20. J. G. Lee, J. H. Lee and H. S. Tae, “Design of a multi beam feed using a nonradiative dielectric Rotman lens”, *IEICE Transaction on Communication*, vol. E85-B, n° 6, June 2002.
21. T. Yoneyama and S. Nishida, “Nonradiative dielectric waveguide circuit components”, *International Journal of Infrared and Millimetre Waves*, Vol 4, No 3, pp 439-449, 1983.
22. T.N.Trinh, J.A.G. Malherbe , R. Mittra,”A Metal-to-Dielectric Waveguide Transition with Application to Millimeter-Wave Integrated Circuits,” *IEEE MTT-S International Microwave symposium* Digest pp-205-207, 1980.
23. H. An, K. Wu, and R. G. Bosisio, “Microstrip line excitation of unidirectional dielectric radiator (UDR) with aperture coupling,” *Asia-Pacific Microwave Conference*, Tokyo, Dec. 6-9, 1994, pp, 79-82.

24. N. Herscovici and D. M. Pozar, "Full-wave analysis of aperture-coupled microstrip lines," *IEEE Trans. Microwave Theory Tech*., vol. 39, pp. 1108-1114, July 1991.

25. W. Grabhard, B. Huder and W. Menzel, "Microwave to waveguide transition compatible with mm-wave integrated circuits*," IEEE Trans. Microwave Theory Tech.*, vol. 42, pp. 1842-1843, Sept. 1985.

26. L. Han, K. Wu, and R. Bosisio, "An integrated transition of microstrip to nonradiative dielectric waveguide for microwave and millimetre wave circuits," *IEEE Trans. Microwave Theory Tech*., vol. 44, pp. 1091-1096, July 1996.

27. A. Bacha, K. Wu, "Toward an optimum design of NRD-guide and microstrip-line transition for hybrid-integration technology," *IEEE Transactions on Microwave Theory and Techniques* Volume: 46, Issue: 11 , pp 1796 - 1800 Nov 1998.

28. Jinbang Tang, Ke Wu, "Integrated microstrip to NRD-guide transition using a spurious mode suppressing technique" *IEEE MTT-S International Microwave Symposium Digest*, June 2000.

29. T.Yoneyama, F. Kuroki, and S. Nishida, "Design of Nonradiative Dielectric Waveguide Filters", *IEEE Trans. On Microwave Theory and Techniques*, Vol. MTT-32, No. 12, pp. 1659-1662, December 1984.

30. J. A. G. Malherbe and J. Corne Olivier, "A Bandstop Filter Constructed in Coupled Nonradiative Dielectric Waveguide", *IEEE Trans. On Microwave Theory and Techniques*, Vol. MTT-34, No. 12, pp. 1408-1412, December 1986.

31. J. A. G. Malherbe and Jacob C. Coetzee, "Bandstop Filter in Nonradiative Dielectric Wave-guide Using Rectangular Resonators", *IEEE Trans. On Microwave Theory and Techniques*, Vol. MTT-35, No. 12, pp. 1161-1163, December 1987.

32. N. P. Pathak, "Linear and non-linear millimetre wave circuit elements using non-radiative dielectric wave guide", *Indian Institute of Technology, Delhi*, 2005.